PART I

INTRODUCTION

PART I - INTRODUCTION

The first part provides an overview to the main topics of this thesis. Chapter 1 deals with hard coatings and plasma technology for materials processing. Several aspects concerning the first steps (history) in protective coatings open this chapter. After that, different hardening mechanisms, their relation with nanostructure, and their implementation in deposition procedures at industrial scale are briefly discussed. These aspects illustrate the motivations and recent trends in hard film research. The second section is an approach to the technological applications of certain kinds of plasmas, namely low-pressure and low-temperature discharges. Further considerations regarding physical aspects of glow discharges are separately described in appendix C.

Diamond-like carbon (DLC) is the topic of chapter 2. There, an introductory section provides general information about carbon, from atomic scale to solid state formations. Amorphous carbon (a-C) is then analysed from the points of view of its physical properties, its synthesis in thin film form, and the great number of applications.

Chapter 1

Introduction

Chapter 1 – Introduction

1.1. Hard coatings: state of the art

1.1.1. History of hard coatings

Since the bronze-age of the antiquity, many efforts have been made towards the realization and further optimisation of hard materials and metals. Later, protective coatings were one of the alternatives applied to iron tools. Among the required properties of the protective materials, good adhesion to the substrate and high hardness are the most representative. A huge research on materials engineering has been made from this period of human evolution up to the current findings of superhardness measured in certain multielemental materials.

The history of hard coatings shows an evolution strongly related with Metallurgy. The formation of hard carbides in layers on the surface was possible at high temperature by diffusion of carbon when red-hot iron was dipped into oil. Former experiments mixing iron with steel provided materials with new properties, although these still required major improvements. The Damascus steel represents a notable stage in this context (figure 1.1).

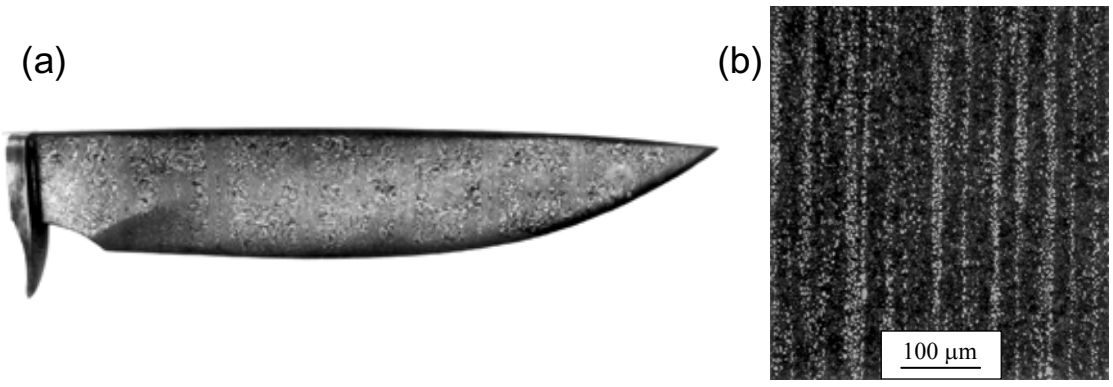

Figure 1.1: (a) A reconstructed wootz Damascus blade showing the Damascene surface pattern containing a combined Mohammed ladder and rose pattern. (b) A longitudinal section of the same blade showing the bands of cementite particles responsible for the surface pattern.

Several thousands of recipes to prepare steels with different properties have filled the pages of Materials Science handbooks since the middle-age. The only constitutive difference among these steels is the element combined with carbon. Depending on this

added element, the resulting material shows certain functional properties. The fact that coated materials show generally superior mechanical properties than uncoated is the supporting point in hard films research. On the other hand, the evolution in hard coatings has been parallel to the deposition technology of thin films. The properties of thin films are somewhat different than the ones shown by material in bulk form, since thickness ($\leq 1\mu m$) is very small compared to the surface dimensions. The first evidences of the production of thin film are gold leafs of 0.3 μm from Luxor (Egypt), which date to XVI-XIV centuries B.C. In the XIX century, the scientific research on this matter passed from metals beating to electrochemical methods. The Faraday experiments provided significant advances in thin film technology through the electrodeposition of metals, in which a major control of deposition parameters was achieved. Thin film preparation was improved by new-coming and cleaner deposition techniques, where high-vacuum conditions are required. Thus, applications of thin coatings spread to new fields as optics and electronic devices. The applications of plasma in modern techniques of film growth are discussed in section 1.2.3.

Chemical vapour deposition (CVD) technique permits growing thin films from gaseous precursors. The first commercialized hard films deposited by the CVD technique date from late 1960s. Sputtering and evaporation -either thermal or electron-induced- of a solid constitute the basic physical vapour deposition (PVD) methods, which were firstly employed for the coating of tools in 1980s. TiN and TiC were then used to coat drills and cutting inserts.

Recent investigations have provided special materials with hardness in the range of diamond (80-100 GPa). The most common compounds employed in hardness applications are basically carbides, nitrides and borides of groups IV, V and VI of the periodic table, namely TiN, TiC, TiCN, TiAlN, CrN, Al_2O_3 (alumina), and more sophisticated combinations thereof. The use of plasma techniques for deposition ensures that only surface is coated, so high brittleness associated to an integral nitriding of the samples is avoided. Aside of these ceramic films, diamond-like carbon (DLC), WC/C and MoS_2 are adequate for lubricating applications due to their excellent tribological properties. Figure 1.2 shows some DLC- and TiN-coated work pieces.

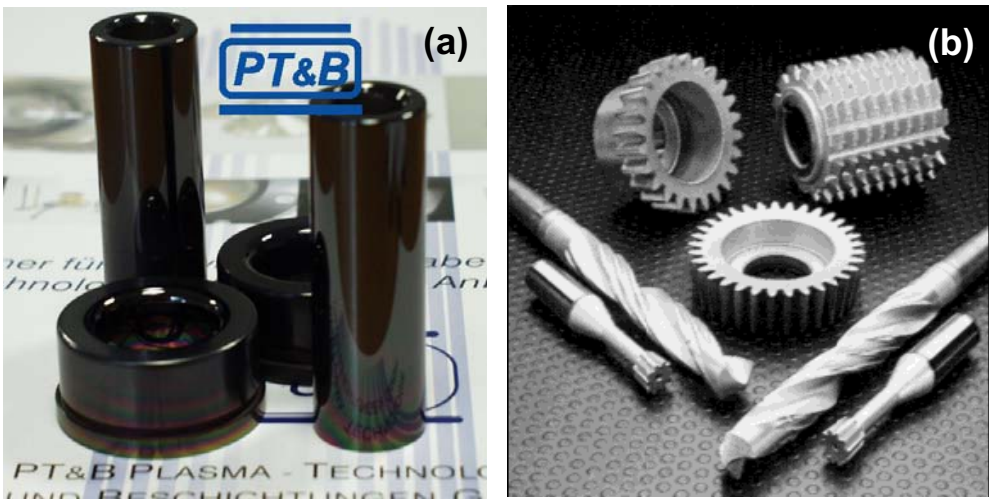

Figure 1.2: (a) DLC and (b) TiN coatings applied to cutting tools.

The present status in the research on superhard coatings involves three different approaches concerning the film preparation [Veprek S., 2005]. The basic idea contemplates the tuning of coating properties by alloying or structuring base materials with new elements:

- Intrinsically superhard materials (diamond, DLC, c-BN)
- Materials hardened by energetic ion bombardment
- Nanostructured hard coatings

In the last group, one must pay special attention to the distribution of material within the film. We can find for example composites and some heterostructures such as multilayers, which constitute one of the main focuses in current research [Hauert R., 2000].

1.1.2. Improvement of mechanical properties

This section continues the explanation of the "state of the art" by commenting some methods to improve the mechanical properties of coatings. According to the approaches in hard coatings research mentioned above, hardness enhancement by means of ion bombardment modulation and self-organized nanostructuring will be discussed.

There are two basic mechanisms that enhance hardness in alloys [Hauert R., 2000]. The first one is the modification of the chemical bonding (TiN). It can be managed by either changing the material added in the alloy or by modifying the stoichiometry. The second option consists in the introduction of lattice distortions (TiAlN), which difficult the

propagation of dislocations through the solid. This is a typical effect in a superhard material, since such materials show minimised dislocation activity. As examples of lattice distortions we can mention grain boundaries, defects, and local stress enhancing. Hence, highest hardness is achieved for maximal concentration of introduced distortions.

Composite ceramic coatings consist in systems with two or more thermodynamically-driven segregated components. The grain boundaries included in these two-phase materials introduce the lattice distortions that increase hardness, which is especially higher for nanometer sized grains. In the case of polycrystalline solids, this hardening effect is expressed through the Hall-Petch relation [Hall E.O., 1951] [Petch N.J., 1953]:

$$\sigma_y = Kd^{-1/2} + \sigma_0 \qquad (1.1)$$

where the enhancement of the yield stress, σ_y, is connected to the grain size, d, by means of two constants, K and σ_0. According to this model, the higher hardness of materials with smaller grain size is ascribed to the pileup of dislocations at grain boundaries. In fact, such defects act as obstacles for dislocation motion through the solid. If the embedded grains are nanoscaled, we can refer to this material as *nanocomposite*. Then, it is said that mechanical properties are improved by superlattice effects. Below 10 nm of grain size, dislocations do not exist any longer in nanocomposites, being then replaced by grain boundary sliding. A superlattice is a solid constructed by two or more superimposed patterns with similar scales. Figure 1.3 shows a scheme of crystalline inclusions embedded in an amorphous matrix as an example of composite material. Here, the grain size coincides with the crystallite size.

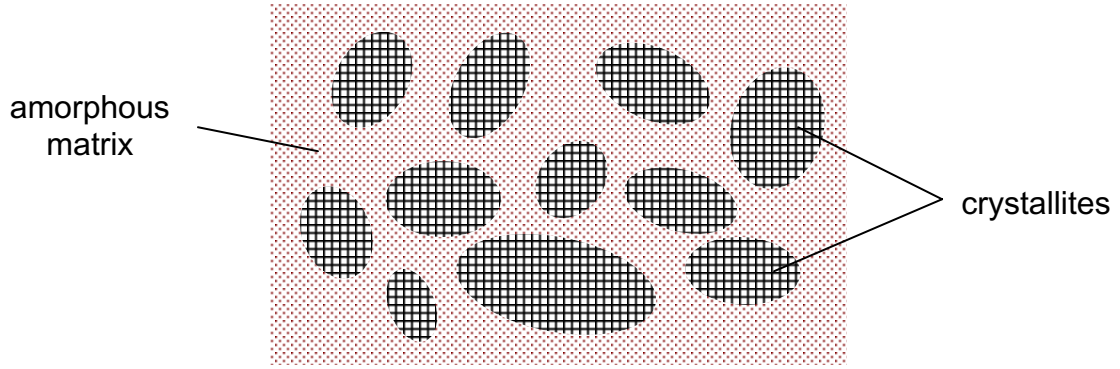

Figure 1.3: Schematic picture of crystalline inclusions within an amorphous matrix.

Hard nanocomposite coatings accept a classification as a function of their structure and the elements therein. According to Musil [2000] two basic groups can be distinguished: crystalline/amorphous and crystalline/crystalline nanocomposites. Seven different types have been prepared until now:

I. nc-MeN/a-nitride
II. nc-MeN/nc-nitride
III. nc-MeC/a-C
IV. nc-MeN/metal
V. nc-MeN or MeC/a-boride
VI. nc-WC + nc-WS_2/DLC
VII. nc-MeC/a-C + a-nitride

From this collection, only nc-MeN/a-nitride and nc-MeN/metal show superhardness, which proves that superhard films can be composed by hard/hard or hard/soft phases, respectively.

Me-DLC films, which have attracted great interest since their initial study two decades ago [Dimigen H., 1987] [Klages C.P., 1989], present a nc-MeC/a-C:H structure. Although it is not superhard, this structure shows advantageous properties in hard coatings technology: deposition at room temperature, low intrinsic stress and improved substrate adherence. These properties suggest the use of Me-DLC in wear-resistant and interficial applications, as for example buffer layers. The preparation and characterisation of Me-DLC films is analysed in chapter 8 of this dissertation.

Multilayer structures are a special case of composites. Building of multilayer structures gives place to coatings with improved hardness and wear-resistance. Multilayering may be due to composition modulation or alternating phases of the same material. Anyway, multilayers presenting a bilayer period below 10 nm show superior mechanical properties due to superlattice effects, as in the case of nanocomposites formed by isotropic phase segregation. Hence, the Hall-Petch formula (equation 1.1) may also be applied. Here, dislocation propagation is hindered by the interfaces that define the structure. Chapter 7 presents the characterization results of metal/carbon multilayers, which show improved mechanical properties with respect to monolithic films.

Multilayer superlattices are expected to work as good protective coatings for many reasons. With them, wear rate considerably decreases because the cracks generated in wear conditions show a minimised penetration depth. For instance, cross-section TEM studies on TiAlN/CrN superlattice coatings showed that columnar hard coatings were plastically deformed and delaminated in an easier way in comparison with multilayer structures [Hovsepian P.Eh., 2000]. Moreover, the interfaces of the layered structure suppose a barrier for oxidation due to the formation of passivation oxide layers. As conclusion, multilayer structures present improved mechanical wear behaviour both at room and high temperatures.

The origin of hardening mechanism in both nanocomposites and multilayer nanostructures is the existence of sharp interfaces between phases. Moreover, these phases must present a large difference in shear modulus. This is the main cause of choosing amorphous materials to lodge nanoinclusions. In fact, any inclusion is well encapsulated by an adaptable amorphous solid rather than by a rigid crystalline network. Sharpness of interfaces enhances the lattice mismatch between layered phases in multilayers, which produce coherency strains in the interfaces. It has also an effect on hardness enhancement, although less intense than the modulation of shear moduli amplitude.

Energetic ion bombardment is another way to obtain hard coatings based for example on nitrides and borides. A determined range of ion energies is selected by biasing the substrate, fact that permits the control of the material properties. However, this method is disadvantageous in the case of coatings that are thermally instable. In fact, their mechanical properties may be degraded upon heating. This supposes an important drawback in industrial applications and in any kind of high temperature-application of these hard coatings. Nevertheless, this is a usual method for hard films deposition.

It is well known that the internal stress shown by thin films contributes to the hardness increase. Mechanical stress of coatings is a consequence of their lack of accommodation on substrates. Extrinsic stress may be introduced by thermal effects or simply by mechanical compression of the substrate. On the other hand, dense coatings grown in high energy bombardment conditions or films that show lattice mismatches in the case of epitaxial growth are typical examples of samples with internal stress. Also called residual stress, it is

classified into compressive and tensile depending on the curvature sign of substrate, which is in turn determined by the forces exercised by the film. The definition of *positive* and *negative* curvature is shown in figure 1.4:

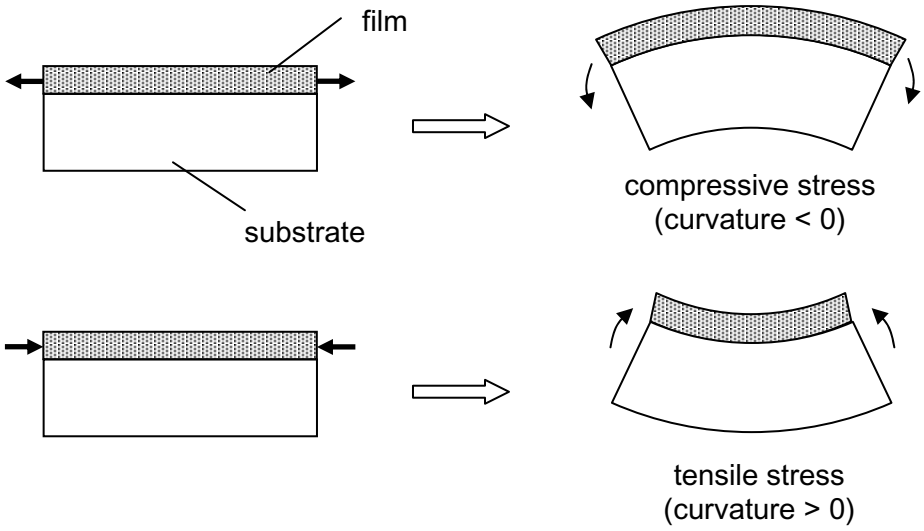

Figure 1.4: Schematic pictures of films under residual compressive and tensile stress. The arrows show the force exerted to the substrate by the deposited film.

The majority of PVD coatings show a large compressive stress due to energetic ion bombardment during deposition. Stress relaxation by maintaining original hardness values is an important issue in material processing, since a good adhesion to substrate cannot be achieved by much stressed films. Otherwise, film cracking and even delamination may occur. Annealing processes posterior to deposition may release this collateral effect. Another solution could be the enhancement of adhesion by depositing a thin buffer layer onto the substrate. Chapter 6 deals with the alternative solution of pulse the plasma to alter the stress of DLC films. Indeed, they show a stress relief due to the obtaining of more relaxed structures. More possibilities consist in varying the composition and even the nanostructure of the material. The latter case may not only reduce stress, but enhances film toughness by promoting grain boundary sliding [Schiotz J., 1998]. This effect will be treated in chapters 7 and 8, where a relationship between structural and mechanical properties of Me/DLC and Me-DLC films will be discussed.

1.1.3. Examples in industry

Hard coatings find applications in all the situations where protection of surfaces in hostile conditions is needed: resistance to wear, corrosion and oxidation, where temperature and

humidity play important roles. For example, TiAlN is a well-known protective coating against oxidation because of the formation of an Al_2O_3 passivation layer on the surface. V is another element that also prevents from oxidation.

Because of the simple structure of intrinsically superhard materials, as for example diamond, the study on their production as thin films is a crucial task. The synthesis of industrial diamond for commercial purposes has been carried out for over 40 years. High-pressure and high-temperature (HPHT) techniques can produce diamond from metal-solvated carbon. The range of pressure is 5-10 GPa, whereas temperature must reach between 1800 and 2300 K. The high cost associated to the infrastructure demanded either the creation of new technologies to prepare it or the search of alternative materials with similar properties. This effort has been prioritised in the past 20 years in hard coatings research; concretely it has focused on diamond, DLC and c-BN materials. A brief list of their applications can be found in chapter 2.

The commercialization of these hard coatings requires that the specific goals imposed by quality controls are reached. Therefore, these coatings must show a progressive improvement in their properties: hardness increase, good substrate adhesion and acceptable tribological properties.

A market research report of Business Communications Company (BCC), Inc., “RGB-173X Diamond, Diamond-like Carbon/CBN Films and Coated Products: Technology Analysis”, was published in 2002. It presents an estimation of the current size and future growth of worldwide markets, focusing on U.S., for the period 2001 through 2006. According to the BCC study, the U.S. market for diamond and diamond-like films in 2001 was $150 million. To have an approximate idea of the importance of DLC coatings and similar, over 70% of this market was attributed to diamond-like thin films, and is expected to continue increasing in the next years.

In the 1980s, Japan and the former Soviet Union showed a status in diamond and diamond-like film technologies more advanced than that of the U.S. Later, the activation of the U.S. in this field permitted the development of new technologies and the improvement of the existing ones, increasing the applications of this research field. The graph of figure

1.5 measures the research activity in DLC coatings by means of the published patents share from U.S., Japan, Europe, and other countries, corresponding to the period of time from 1995 to 2004.

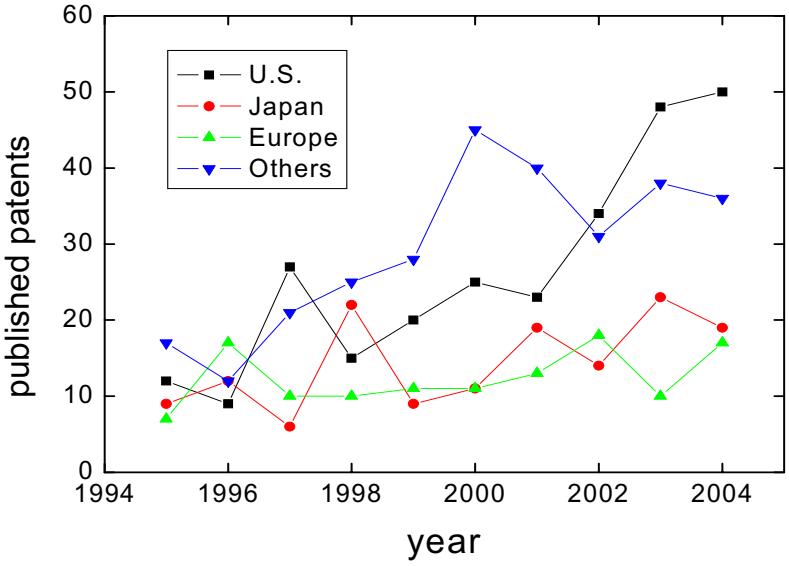

Figure 1.5: Evolution of patents in DLC issued to the U.S., Japan, Europe and other countries.

Figure 1.6 shows a pie diagram to compare status in 1996 and 2004. After the minimum of 18% reached by the U.S. in 1996, its contribution started to increase until 41% in 2004. On the opposite, Japan's and Europe's indexes experienced a smooth decrease during this period, from 24% and 34%, to 15.5% and 14%, respectively. Several countries as South Korea, Canada and Taiwan leaded the considerable increase of the rest by providing a combined share of 29.5% in 2004.

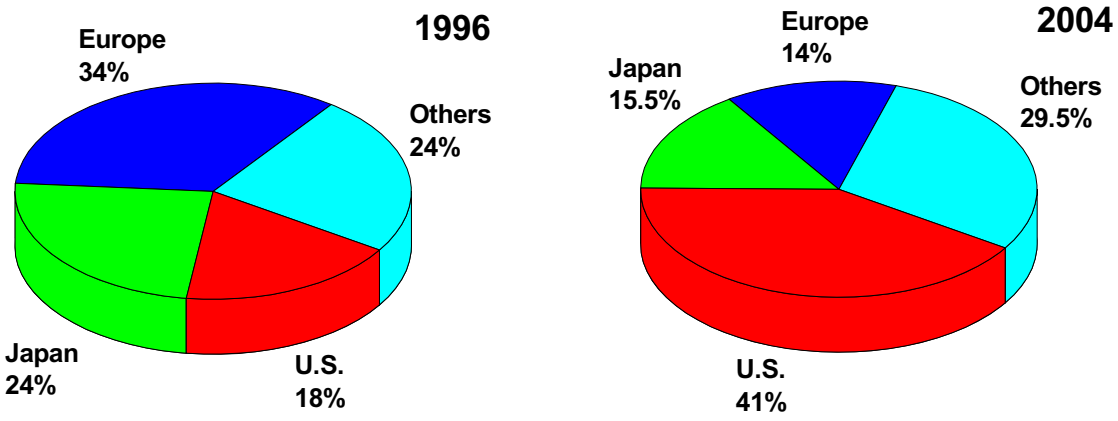

Figure 1.6: Pie diagrams showing the status in 1996 and 2004 of the patents in DLC.

Now, we focus on concrete examples of hard films. Superlattice structured coatings show two or more superposed lattices. These structures are suitable for protective coatings applications if their thickness ranges within the micron range. Actually, Japanese and British cutting tool manufacturers have implemented in the market the multilayered coating of cutting tools. In the late 1980s, nanoscale compositionally modulated multilayer structures showed a great progress, and current research deals with structures presenting bilayer periods or wavelengths down to 2 nm. Nowadays, there is a clear predominance of TiN-based superlattice coatings, as for instance TiN/WN, TiN/CrN, TiN/TaN, TiN/MoN and TiN/AlN. These structures are grown by combining magnetron sputtering and arc evaporation techniques. More complex structures like TiAlN/CrN and TiAlYN/VN are being investigated.

Multilayer structured coatings require special deposition setups in order to be properly prepared. The sputtering multi-target geometry deposition equipments suppose a popular configuration to this end. The use of commercially available HTC 1000-4 PVD system with 4 rectangular sputtering cathodes has been described in several reports [Bewilogua K., 2000] [Hovsepian P.Eh., 2000], although other systems with similar architecture are also available [Lampe Th., 2003]. Figure 1.7 shows a schematic cross-section of this coating plant. The rotation of the substrate-holder leads to the deposition of composition-modulated structures in a reproducible manner.

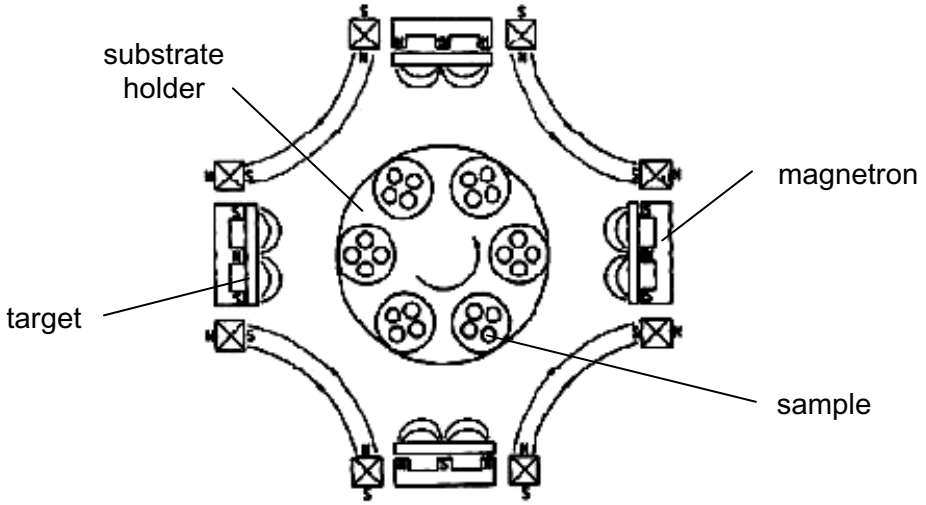

Figure 1.7: Schematic diagram of the four cathode HTC 1000-4 PVD coating equipment [Münz W.-D., 2001].

Attending concrete applications of hard multilayers, TiAlYN/VN structure triples the lifetime compared with TiCN coated tools. This conclusion is extracted from a wear study of flute ball nosed cutters [Münz W.-D., 2001]. The system CrN/NbN shows a successful application on forming tools, as well as promising properties for cutlery industry (coated knife plates). Such structure is also indicated for automotive engine guide valves. Indeed, their lifetime increases considerably after coating. Further studies point to more promising applications of multilayer structures in components used in the textile industry such as combing rolls.

Other interesting nanostructured materials are nanocomposites. They consist on a crystalline phase formed by crystallites, which are embedded in an amorphous matrix. These crystalline inclusions have a grain size in the nanometer range and they follow a random distribution within the matrix. Both phases become segregated owing to their complete immiscibility and they are simultaneously deposited during film growth. Very known examples of nanocomposites are the Ti-Si-N and Ti-B-N systems, being TiN/Si_3N_4 the most important.

The first coatings containing Ti-Si-N were produced by CVD in 1982. Later, they were identified as nc-TiN surrounded by a matrix of a-Si_3N_4, which exhibited a maximal hardness of around 50 GPa. Unfortunately, the gases involved in deposition were hazardous: $TiCl_4$, SiH_4, H_2 and HCl, which difficult the process engineering. This drawback was solved by co-depositing this nanocomposite by reactive sputtering from Ti and Si targets.

Other nanocomposites that exhibit the isotropic morphology identified in TiN/Si_3N_4 are nc-TiN/a-BN, nc-W_2N/a-Si_3N_4, nc-VN/a-Si_3N_4 and nc-$(Al_{1-x}Ti_x)N$/a-Si_3N_4. Some of these nanocomposites have been prepared in large-scale industrial coating plants, where a high control of impurities must be held because their presence degrades the mechanical properties. The most negative effect in this way is introduced by oxygen impurities, which avoid reaching the superhardness threshold (40 GPa). Besides diamond, the top-values of ultrahardness have been achieved by ternary and quaternary nanocomposites: 70-80 GPa in nc-TiN/a-Si_3N_4/a-$TiSi_2$, and 100 GPa in nc-TiN/a-Si_3N_4/a-$TiSi_2$/nc-$TiSi_2$.

As well as in the case of nitrides, extensive studies on carbide particles embedded in DLC have also been made. The doping of DLC with metallic elements, as Nb, Ti or W, leads to structures presenting carbide nanocrystals distributed within the amorphous DLC matrix. Metal-containing DLC (Me-DLC) films exhibit hardness values above 30 GPa, and their structure and outstanding properties have been reported in many papers [Schiffmann K.I., 1999] [Precht W., 2003]. Chapter 8 of this thesis is a contribution on the study of Me-DLC films. The discussed metals are Mo, Nb, Ti and W.

The quality tests are the last stage in industrial production of protective films. The results decide whether a determined coating is accepted to be commercialized. In this step, the samples are subjected to simulated environments, which demand the employment of selected substrates. For instance, cemented carbides are suitable for high temperature tribometry, whereas 304L stainless steel is usually assigned for structure and corrosion resistance measurements. The testing and characterisation protocols comprise several techniques, some of which are described in chapter 4: micro- or nanoindentation for hardness determination, substrate adhesion by scratch test, residual stress by profilometry or X-ray diffraction (XRD), transmission and scanning electron microscopy (TEM, SEM) and XRD for microstructure, pin-on-disk for wear rate, thermo-gravimetric analysis to evaluate oxidation resistance, and corrosion evaluated by electrochemical methods.

1.1.4. Future trends

Further investigations point to the ever-growing need to develop hard coatings for tribological applications, long-life coatings and high temperature performances. Biomedical implants are an example of other applications in which a correct functionality is critical. For this purpose, a deep understanding of hardening mechanisms on materials must be achieved.

The importance of synthesizing multicomponent materials is that their final properties are controlled by the mutual interaction of the components. Thus, the combination of several elements may lead either to new materials or to multi-phase composites with physical properties tuneable by the technological parameters.

The topic material of this thesis, DLC, constitutes an appropriate base material for alloying with elements and, thus, for tailoring its basic properties because inclusions are more adaptable to amorphous structures. Some examples of additional elements in DLC alloys are Si, N, O, W and Ti. The aim of alloying DLC is enhancing its most remarkable properties, namely tribological and biocompatibility properties. The role of energetic ion bombardment to achieve superhardness in thin films is another remaining issue.

Currently, there is a lack of knowledge in the effect exerted by the interaction between materials on the mechanical properties. The main challenge is to predict the effect of basic properties and microstructure of a material on its functional properties. Therefore, future work is intended to elucidate more about these correlations. This deeper knowledge may lead to the production and development of hard coatings with superior mechanical and tribological properties.

1.2. Low-pressure plasma technology: state of the art

1.2.1. Definition and history. Plasmas in the nature

The intuitive concept of plasma is usually a light-emitting gas, which is only a special case of plasmas. The general features of plasmas are electric quasi-neutrality and the existence of free ions and electrons. Thus, the presence of ions leads to particles having excited states, which in turn increase the energy of some charged particles due to the action of collisions, electric and/or magnetic fields, and other processes. These phenomena have been registered from reactors in laboratories to some spontaneous processes in nature. Actually, plasmas are present in many regions of the Universe. As examples, we can remark fluorescent tubes, the ionosphere, and stellar and interstellar media. In order to achieve the plasma state, some special conditions must be fulfilled.

Since the invention of a new vacuum pump by Geissler in 1855, some experiments of gas discharge in low pressure tubes were performed by many scientists (Goldstein, Crookes and Hertz among others) in the second half of XIX century. They observed the formation of diverse glow fringes between the electrodes in the tube, whose colour was related to the employed gas. Figure 1.8 depicts a gas discharge tube. It contains two facing electrodes, where the cathode is the electron emitter and the anode receives the electrons. This electronic current is called cathode rays and it produces a succession of dark and glow spaces, whose respective luminosity and separation depends on the applied voltage, the gas inlet and the pressure.

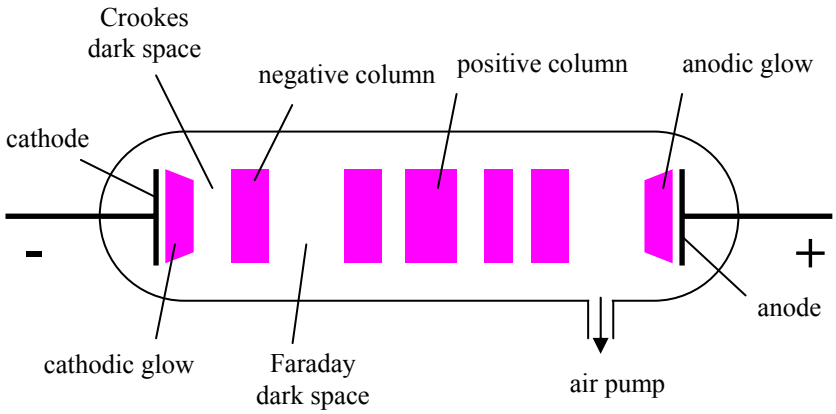

Figure 1.8: Scheme of a cathode rays tube, showing the different gas discharge regions.

At low enough pressures (< 0.15 Pa), fluorescence was detected around the anode. In 1895, Röntgen found that an invisible component of this radiation was able to pass through opaque objects and mark photographic plates. Because he ignored the nature of this radiation, he called it X-rays, which constitute the basis of the radiography technique. Further studies performed by Sir J.J. Thomson on the properties of this electronic flow between the electrodes led to the discovering of the electron and, as a consequence, to the first theories of the atomic structure.

Plasma can be defined as partially ionised system, which shows electrical quasi-neutrality (neutrality on the average, but not close and around a charged particle). It has been identified as the 4^{th} state of matter, along with solid, liquid and gas states. Irving Langmuir gave a more extended definition for plasma, which accounts for its composition and its behaviour in front of external perturbations. According to his concept, plasma is an electrically neutral ionised gas composed by an equivalent number of free ions and electrons, which exhibits a collective response induced by electric and magnetic fields [Langmuir, I., 1928].

As shows figure 1.9, plasmas are classified depending on their parameters (see appendix C). Moreover, these operating regimes arise from the consideration of natural, research and industrial plasmas. Thermonuclear fusion processes develop thermal plasmas, which reach temperatures of about 10^4 eV at pressures lower than 10^{-1} Pa. Thermal plasmas also take place in high-pressure electric arcs. There, electrons at 0.1-2 eV reach a density between 10^{14} and 10^{19} cm^{-3} at atmospheric pressure.

By the context of this thesis, we shall only consider low-temperature and low-pressure plasmas (chapter 5) due to their application in material processing, which comprises film deposition, etching and surface modification. Such plasmas belong to the group of cold plasmas. Table 1.1 lists the range of plasma parameters.

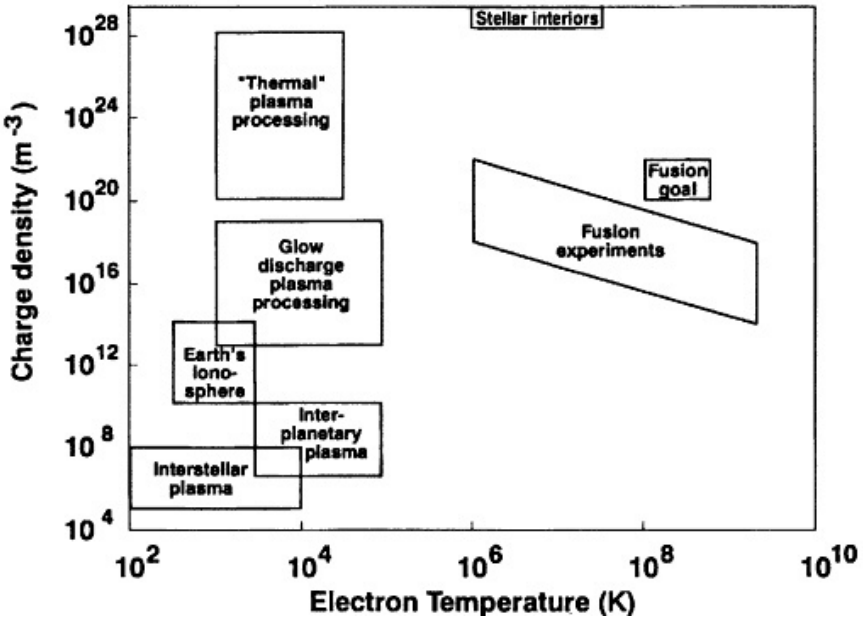

Figure 1.9: Classification of plasmas as a function of charge density and electron temperature [Liebermann M.A., 2005].

Electron temperature	1 – 10 eV $> 10^2$ T_i
Gas temperature	0.03 eV
Electron density	$10^8 – 10^{13}$ cm^{-3}
Ionisation degree	$10^{-8} – 10^{-3}$
Pressure	0.1 – 100 Pa

Table 1.1: Typical ranges of plasma parameters for low-pressure glow discharges [Liebermann M.A., 2005]. The enhancement of the ionisation degree up to 10^{-3} can be achieved by installing a magnetron.

Plasmas are composed by neutral and charged species. Neutrals are molecules, atoms, free radicals and meta-stable species; on the other hand, electrons, positive and negative ions compose the ensemble of charged species.

1.2.2. Generation of a glow discharge

Let us consider the capacitive configuration of electrodes schematized in figure 1.10, which could represent a process chamber. After stabilizing the gas pressure, the application of a voltage between the electrodes promotes the collision between electrons and molecules from the gas. If the generated voltage is high enough, electron sources such as ionisation and secondary electron emission from the cathode increase the electron population so much, that charge carriers are multiplied through an avalanche process. Then, a discharge regime is achieved, thus indicating that plasma has been ignited in a capacitive configuration.

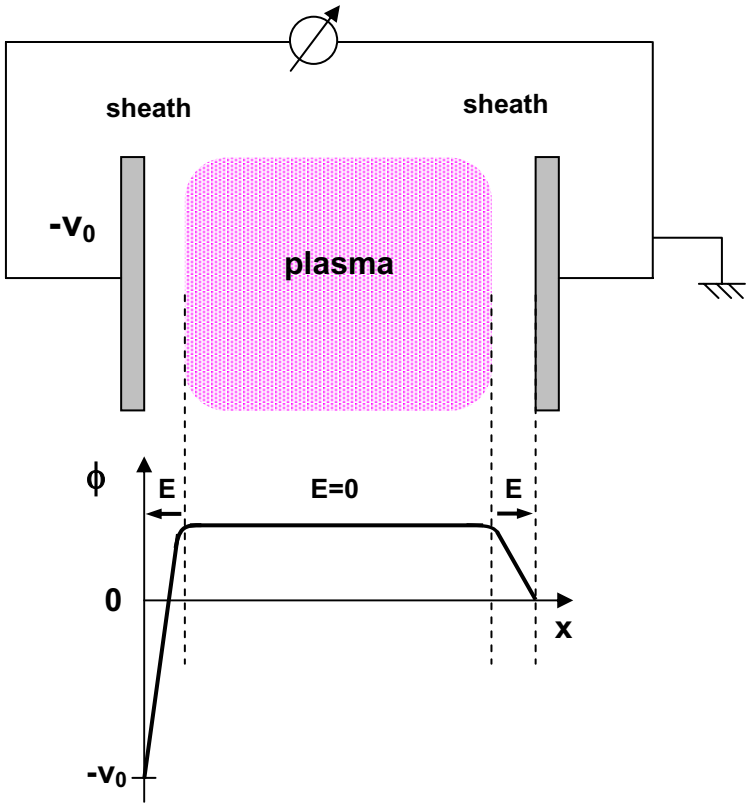

Figure 1.10: Plasma generated in a capacitive configuration. The electric field associated to the sheaths promotes ion bombardment onto the electrodes.

Figure 1.10 also plots qualitatively the potential profile along the *X*-direction. The flat region indicates that the electric field is null in the plasma bulk. However, it is only true at a scale greater than Debye length, where any variation of electric potential is screened by the spatial charge distribution, as explained in appendix C. The absence of electric forces therein yields to electrons and ions to follow the kinetics of a gas of free particles.

The potential drops are spatial charge distributions that occur near the walls. They are called *plasma sheaths*, and appear as a consequence of the major mobility of the electrons in comparison with the mobility of the "heavy" ions (see appendix C). Owing to this potential gradient, an electric field points from the plasma bulk to the walls. This potential profile results in a potential valley for electrons and negative ions, and a potential hill for positive ions. In other words, positive species are accelerated from sheath-edges to the walls, whereas negative species (electrons and negative ions) are confined within the glow discharge.

The breakdown voltage, V_b, is the voltage necessary for the discharge to be self-sustaining. It can be evaluated with this formula [Roth J.R., 1995]:

$$V_b = \frac{Bpd}{\ln Apd - \ln[\ln(1+1/\gamma_{SE})]} \tag{1.2}$$

A and B are empirical parameters, p is the gas pressure, d is the gap between electrodes, and γ_{SE} is the secondary electron emission coefficient of the cathode. The curve $V_b(pd)$ is called the Paschen curve, and shows a minimum at some intermediate values of pd. Indeed, extreme values of pd are prohibitive for plasma existence.

· Plasma sheaths

The last explanations described plasma phenomena in bulk. However, bounded plasmas exhibit spatial charge regions in their edges. As commented above, these regions show a non-uniform potential that generate an electric field, which in turn accelerates positive ions towards the walls and reflects negative species.

Some models of plasma sheaths have been developed. Equation 1.3 provides the sheath potential, ϕ, and ion and electron densities in a collisionless sheath [Liebermann M.A., 2005]:

$$\frac{d^2\phi}{dx^2} = \frac{en_s}{\varepsilon_0}\left[\exp\frac{e\phi}{kT_e} - \left(1-\frac{e\phi}{\xi}\right)^{-1/2}\right] \tag{1.3}$$

where n_s is the electron or ion density at the sheath edge, T_e is the electron temperature, e is the elementary charge ($1.602\cdot10^{-19}$ C), k is the Boltzmann constant ($1.38\cdot10^{-23}$ J/K), and ξ is the initial ion energy. Usually, sheath voltages show values larger than T_e. In this case,

sheath thickness can be estimated by using the high-voltage approaches of matrix sheath or Child Law sheath. These approximations point to thicknesses between 10 and 100 times the Debye length, while smaller values as pressure increases are observed in collisional sheaths.

The role of plasma sheaths in material processing is critical. The samples to be treated are placed in the boundary regions of plasmas. Therefore, ion bombardment in sputtering targets, deposition of atoms, ion etching and ion implantation are governed by the shape and the potential drop of the sheaths. Some applications in which plasma sheaths are directly involved are described in section 1.2.3.

· Basic processes

Through accumulation of real-time monitoring of plasma parameters, a rich diversity of chemical processes has been collected. The most significant phenomena involving reactions among plasma species have been summarized with some examples [Ohring M., 2002]:

1. Ionization: $e^- + Ar^0 \rightarrow Ar^+ + 2e^-$
2. Excitation: $e^- + O_2{}^0 \rightarrow O_2{}^* + e^-$
3. Dissociation: $e^- + CF_4 \rightarrow e^- + CF_3{}^* + F^*$
4. Dissociative ionization: $e^- + CF_4 \rightarrow 2e^- + CF_3{}^+ + F^*$
5. Electron attachment: $e^- + SF_6{}^0 \rightarrow SF_6{}^-$
6. Dissociative attachment: $e^- + N_2{}^0 \rightarrow N^+ + N^- + e^-$
7. Symmetrical charge transfer: $A + A^+ \rightarrow A^+ + A$
8. Asymmetric charge transfer: $A + B^+ \rightarrow A^+ + B$
9. Metastable-neutral: $A^* + B \rightarrow B^+ + A + e^-$
10. Metastable-metastable ionization: $A^* + A^* \rightarrow A + A^+ + e^-$

Opposite from recombination, ionization is produced due to electron impacts and is critical in the self-sustaining of plasmas. The Ar ionization is a typical reaction in glow discharges for sputtering processes, as explained in section 1.2.3. On the other hand, less energetic electron impacts are not able to ionize, but excite a molecule to higher energy states. In dissociative processes, the target molecule is broken in smaller fragments (radicals), which participate in further plasma reactions.

1.2.3. Application to film deposition

Material processing by chemically active plasmas is a basic tool in the manufacturing industry worldwide [Lieberman M.A., 2005]. Plasma-based techniques for surface modification present the great advantage of controlling surface features up to the nanometer scale. Material fabrication in thin film form, plasma-immersion ion implantation (PIII) [Anders A., 2000], and plasma etching for lithography or just surface cleaning are the main processes that make plasma treatment so attractive in Materials Science. Deposition of protective coatings and films with optical and/or electric performance are examples of the versatility of plasma techniques. Large-scale fabrication of integrated circuits in the electronic industry is one of the most benefited processes by the plasma technology. Other involved industries are aerospace, automotive [Lampe Th., 2003], steel and biomedical [Hauert R., 2004]. Table 1.2 is an outline of the main plasma applications:

Surface treatment	Ion implantation Plasma cleaning Plasma arc (torch) for cutting Plasma etching (lithography)
Material synthesis	Sputtering Plasma CVD Plasma spraying
Volume processing	Waste treatment Instrument sterilization Water purification
Light sources	Gas tubes High intensity discharge lamps

Table 1.2: List of plasma applications.

Thin films can be deposited by plasma techniques in a secure way. Operators must take care only in a few points about safety. One of them consists in the use of hazardous, toxic or environmental non-friendly gases, as for instance SiH_4 or B_2H_6 (flammables) for PECVD films. Deposition set must be then prepared with a proper vacuum line to expel the residual gases to a safe place. Another issue for safe operation is the prevention from electrical shocks, since high voltages associated with power supplies are normally involved.

Plasma-enhanced CVD and sputtering techniques for thin film growth have been the techniques employed in this thesis to deposit thin film structures of DLC. The accurate tailoring of coating properties and a high reproducibility of deposition conditions are achieved by controlling a great number of technological parameters. These deposition methods are briefly described below.

· SPUTTERING

This plasma-based PVD technique is specially used in the fabrication of contacts and the preparation of oxide films. [Ohring M., 2002] [Rossnagel S.M., 2003]. In 1852, Grove found that a cathodic sputtering was characteristic of glow discharges. This means that cathode was progressively sputtered by the plasma as long as the discharge regime was sustained. Sputtering consists in material extraction from a cathode by ion bombardment onto its surface. The origin of the bombarding ions define two types of sputtering process: plasma and ion beam-assisted sputtering. Here we deal with the former. Film deposition can be performed by placing a target material onto the cathode surface and by fixing a substrate near to this target. Thus, particles emitted from the target are able to coat the substrate. A scheme of the usual chamber geometry used for sputtering depositions can be found in section 2.2.

The sputtering process is based on the momentum transfer between colliding particles from plasma and the particles of the target. The ion-surface interactions lead to different phenomena, namely ion cascade, implantation and knock-on. Figure 1.11 summarizes these three processes.

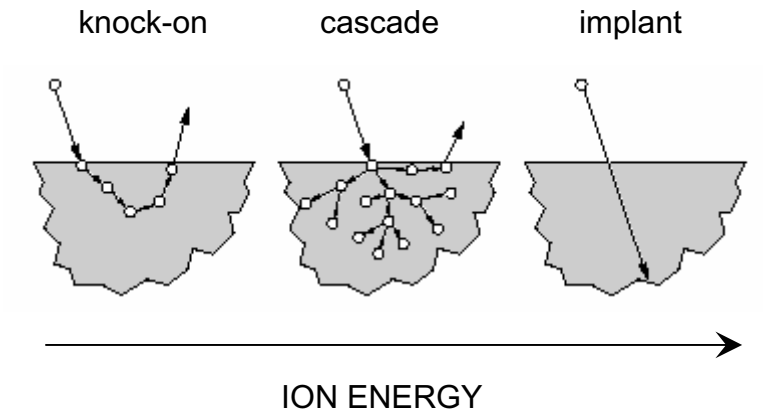

Figure 1.11: Schematic of the three basic processes in ion-surface interaction during sputtering, at different ion enegies.

Three regimes of sputtering can be distinguished if we attend to the kinetic energy of the projectile particles [Rossnagel S.M., 2003]. The knock-on regime is manifested between 10 and 1000 eV of projectile energy and is of interest for deposition purposes. As the energy of impinging particles increases, knock-on regime passes to cascade collision. Although this regime leads generally to a maximum of sputter yield, operating in such regime may damage the target material due to a significant large-scale rearrangement of atoms. In the keV range, the scattering cross-section decreases so much that the projectile is implanted in the target material and, then, cascade only occurs at deep target regions.

A fundamental parameter to maximise in sputtering is the sputter yield, *S*. This parameter is defined as the number of atoms or molecules ejected from a target surface per incident ion. It accounts for the efficiency of energy transfer between plasma ions and atoms from the target. Although sputtering yield data have been systematically tabulated, the sputter yield can be written as follows for incident particles having low energies (E_1 < 1 keV) [Ohring M., 2002]:

$$S = \frac{3\alpha}{4\pi^2} \frac{4M_1M_2}{(M_1+M_2)^2} \frac{E_1}{E_b} \tag{1.4}$$

where α measures the efficiency of momentum transfer in collisions; M_1 and M_2 are the masses of the gas particles and target atoms, respectively; E_1 is the energy of incoming ions, and E_b is the binding surface energy. Additionally, for higher energies (E_1 > 1 keV):

$$S = 3.56\alpha \frac{Z_1Z_2}{Z_1^{2/3}+Z_2^{2/3}} \frac{M_1}{M_1+M_2} \frac{S_n(E)}{E_b} \tag{1.5}$$

where Z_1 and Z_2 are the atomic numbers of the respective species; and $S_n(E)$ is a function of energy, masses and atomic numbers of the involved atoms, which accounts for energy loses per length unit due to nuclear reactions.

Emitted particles from the target as consequence of sputtering are mainly neutrals. Approximately 10% of sputtered species are secondary electrons, which contribute to sustain the glow discharge and heat the substrate. In a lower degree, sputtering targets also emit secondary ions, UV-visible radiation and absorbed gases. Gas desorption supposes a contamination source for the growing film.

Sputtering targets can be powered by direct-current (DC) or alternated-current (AC) signals, depending on the conductivity of the target. Indeed, sputtering of insulators require AC voltages in order to avoid charge-up of the target: the charging-up in a given semi-period is neutralized by the incoming charge carriers of the next semi-period. To this end, signals in the radio-frequency (RF) range are normally used. Pulsed-DC sputtering lies in a lower interval of frequencies, 1-500 kHz, which is the so-called middle-frequency (MF) range. The allowed frequency to generate RF-plasmas is 13.56 MHz. Despite the oscillating cathode bias, the RF-sputtering of targets is possible due to the generation of a self-bias in the plasma sheath close to cathode. This happens due to the major electron mobility in comparison with ions.

Under some circumstances, say low pressure in process or reduced sputter yield of targets, the deposition rate of films decreases. Then, the *magnetron* sputtering technique is employed, which consists in placing a magnetron behind the target in order to enhance the sputter erosion rate. In fact, the magnetic lines confine the plasma electrons, increasing notably the ionisation rate. The major concentration of ions in front of the target increases the ion bombardment and, therefore, the velocity of material extraction. Depending on whether the magnetic flux of the central pole exceeds or equals the one of the lateral pole, one can refer to *unbalanced* or *balanced* magnetron sputtering, respectively (figure 1.12). In the first case, the growth process becomes more energetic because it is assisted by the flow of electrons trapped by the magnetic field lines that reach the substrate position.

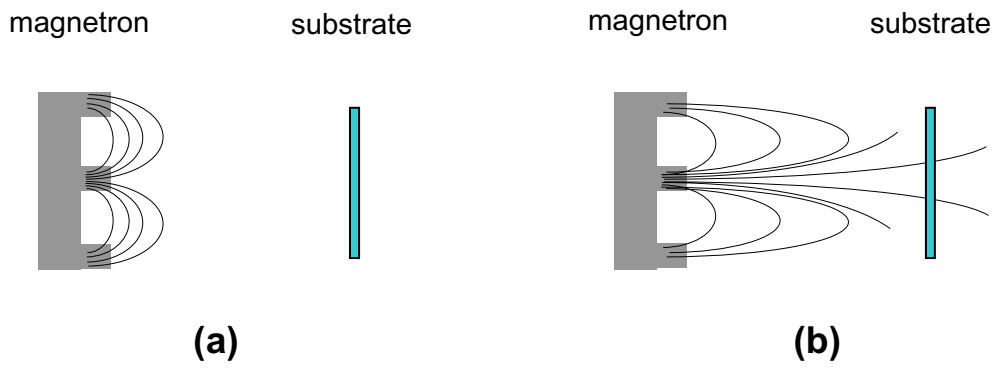

Figure 1.l2: Configuration of a (a) balanced and (b) unbalanced magnetron.

Magnetron sputtering is the most suitable deposition technique to obtain nanocrystalline materials. This method conciliates a high nucleation rate with a low growth rate for grains, which is necessary for grain crystallization [Musil J., 2000]. The results from chapter 8 show that Me-DLC films grown by reactive magnetron sputtering contain nanocrystalline inclusions of less than 10 nm size.

The bombarding ions come from a noble gas (Ar, Kr). In order to deposit materials presenting a composition modified with respect to the target, additional gases that can chemically react with the growing film are admitted in the process. This sputtering variant is called *reactive* sputtering, which admits either DC or RF power supplies. Furthermore, reactive sputtering by means of pulsed-DC supply is a modern method to prevent arcing and contamination of target materials without modifying significantly the film deposition process with respect to the DC technique [Berg S., 2005]. In this thesis, the deposition of Me-DLC films has been realised by pulsed-DC reactive magnetron sputtering of pure metal targets.

Bias-sputtering is a variant that consists in modulating the energy and the flux of incident ions by biasing electrically the substrate. A negative bias is normally imposed; it leads to the reflection of electrons and to the enhancement of the bombarding ion energy. The substrate-holder can be biased to 0 V by grounding it, i.e. by connecting this electrode to the chamber, which operates as anode. On the other hand, if the substrate-holder is insulated from the chamber walls it can be set to floating configuration. Note that substrates are then biased to the plasma potential. The application of negative voltages has

an effect on many film properties (structure, morphology, adhesion). Through the variation of the structural parameters, one can tailor the functional properties in view of the specific coating application.

· PLASMA-ENHANCED CVD

There are two types of CVD processes, depending on the energy source that activates the gas species [Ohring M., 2002]. The film synthesis in *thermal CVD* processes is carried out by supplying heat to the substrates in order to promote reactions and deposition of the material. Such technology comprises atmospheric-pressure CVD, low-pressure CVD (LPCVD), metalorganic CVD (MOCVD), and laser-enhanced CVD. The other technique is *plasma-enhanced CVD* (PECVD), which has been used in this thesis. In this deposition method, chemical reactions are held in a glow discharge or plasma sustained by an electric power supply within the chamber.

The principle of the PECVD technique is the chemical reaction in vapour phase of the constitutive elements in plasma to form material precursors. Thin film growth is performed when the precursors condense onto the substrate. The chemical reactions, which also occur on the substrate surface, comprise basically decomposition, oxidation-reduction, hydrolysis, polymerization, and transport phenomena. PECVD technique is typically used for the deposition of elemental materials (Al, a-C, c-Si), nitrides (AlN, Si_3N_4) and carbides (BCN, SiC).

Like in the case of cathodic sputtering, the type of signal (DC or RF) driven to the cathode determines the nature of PECVD processes. One must drive an alternating bias if the deposition of an insulating material is desired. By either setting a bias or achieving a self-bias at the substrate, the formed plasma sheaths are responsible of the ion bombardment that yields surface covering. Figure 1.10 gives an approximate idea of a PECVD reactor. There, substrates would be fixed on one of the electrodes. In this thesis, the plasma reactions have been activated by driving either RF-generated or pulsed-DC signals to the substrate-holder, which operated as cathode. Chapter 5 deals with the plasma parameters of a methane glow discharge, and demonstrates that their values are influenced by the type of the excitation signal.

PECVD processes can be distinguished by the type of coupling. The *inductively-coupled* configuration is achieved by wrapping a coil around a tube, where the reactions take place. Electrode plates are used in *capacitively-coupled* discharges, where the difference in electrode areas, A_1 and A_2, implies that the formed sheaths provide voltages V_1 and V_2 on the electrodes. This diode configuration obeys the following empirical expression:

$$\frac{V_1}{V_2} \approx \left(\frac{A_2}{A_1} \right)^q \tag{1.6}$$

with the exponent q around 2.5 [Liebermann M.A., 2005]. In order to maximise the cathodic voltage, the walls of the grounded process chamber constitute the anode. This effect is called asymmetrical discharge and justifies why the depositing film is subjected to a more intense ion bombardment when placed on the cathode.

Important to mention are the high-density plasma (HDP) reactors, which are generally used in the deposition of integrated-circuits and etching processes. Electron cyclotron resonance (ECR) technique makes use of a static magnetic field to couple microwave energy to the resonant frequency of the plasma electrons, with the aim to reach high electron densities ($> 10^{10}$ cm^{-3}) in processes without electrodes and at low pressure (10^{-3} to 10^{-1} Pa). The degree of ionisation in ECR is thus about 100-1000 times higher than in RF plasmas.

The basic steps in any CVD process have been summarised in the following list [Ohring M., 2002]:

1. Transport of the reactants from the gas inlets to the reaction zone.
2. Reactions in vapour-phase that form the gas precursors of the film and by-products.
3. Transport of the reactants and their products from the gas phase to the substrate.
4. Adsorption of these species on the substrate surface.
5. Surface diffusion, chemical reactions and incorporation of these species on different growth sites.
6. Desorption of the volatile by-products of surface reactions.
7. Transport of the by-products away from the reaction zone.

All these processes have a strong influence on the properties of the deposited films. Since plasma is the central point of PECVD, the growth process shows an important dependence of the reactor shape and of the technological parameters. For example, the chamber geometry and the gas inlet zone determine the film homogeneity and the growth rate.

Chapter 2

Diamond-like carbon

Chapter 2 – Diamond-like carbon

2.1. Fundamentals and properties

2.1.1. Carbon

Carbon is an abundant chemical element in nature. It constitutes one of the basic elements for life and is widely used in industry for materials manufacturing. The fundamental feature of carbon is its unique capability for combining with other elements. The so called hydrocarbons are formed by the grouping of carbon and hydrogen atoms either in chains (polymers) or in rings (benzene). The addition of methyl radicals, nitrogen, oxygen and other new elements provides more complex molecules (acids, alcohols), whose accumulation leads to polymeric structures. The polymer industry has reached a great development exploiting this technology. This simple image of matter construction permitted in the XIX century to establish Organic Chemistry as a mastered scientific discipline. Since then, one can reproduce in laboratories several substances generated in principle only by living entities. Already in 1828, Friedrich Whöler demonstrated this principle by synthesizing urea.

In order to understand why carbon achieves such an elevated coordination degree, we must study its electronic structure. Carbon occupies the 6^{th} position within the Periodic Table, which provides an electron configuration of $1s^2\ 2s^2\ 2p^2$. Figure 2.1 shows a scheme of the electron distribution in orbitals, where the arrows indicate the spin polarization.

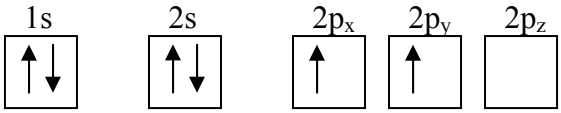

Figure 2.1: Electron distribution in the carbon orbitals for a carbon atom with valence number 2.

The subindexes *x*, *y* and *z* indicate symmetry of *p* orbitals with respect to the corresponding axis (figure 2.2). This differentiation is not required in *s* orbitals, since they are spherical.

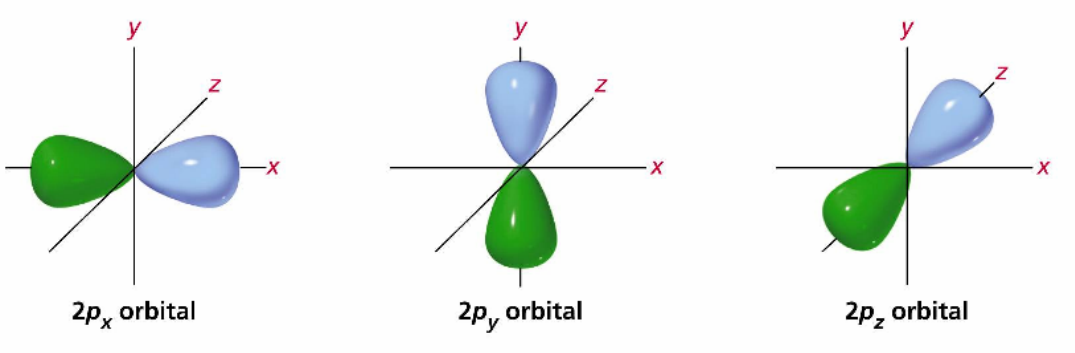

Figure 2.2: Spatial orientation of the atomic orbitals *p*.

Electronic orbitals of the carbon atom contain only two unpaired electrons, behaving thus as bivalent element. In order to justify the tetravalence of carbon, one of the two electrons from the 2s orbital must occupy an empty 2p orbital, resulting in the scheme of figure 2.3.

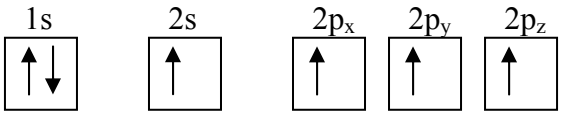

Figure 2.3: Alternative electronic configuration that provides tetravalent carbon atoms.

As a result of the previous redistribution, carbon has four dangling bonds and all the electrons in the outer layer are unpaired. Then, the linear combination of *s* and *p* atomic orbitals generates the so called hybrid orbitals. Hybridisation comprises three cases. The *s* orbital together with one *p* gives rise to two *sp* orbitals. When two *p* orbitals are added to *s* we obtain three sp^2. Finally, the hybridisation of all the orbitals from the second layer provides four sp^3. The generation of the hybrid orbitals is depicted in figure 2.4.

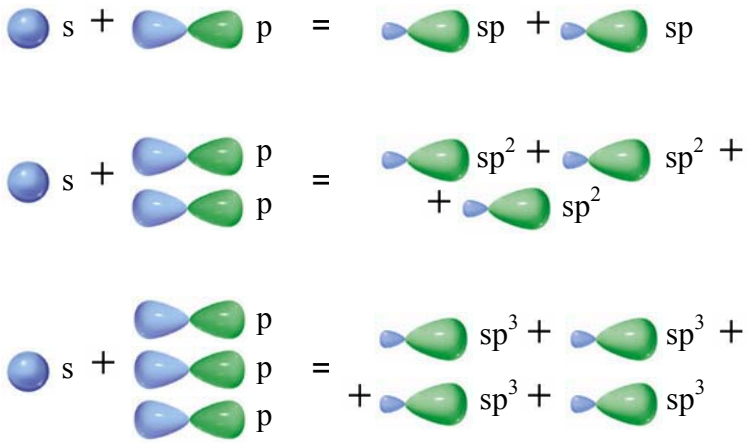

Figure 2.4: Linear combination of atomic orbitals and the resulting hybridisations.

Figure 2.5 shows the possible geometric configuration in the carbon atom depending of the type of hybridisation. Diametrically opposed orientation takes place in the case of *sp* orbitals. In this configuration, both *sp* orbitals make strong frontal σ bonds to an adjacent atom, whereas there are two weak lateral π bonds with neighbouring *p* orbitals. On the other hand, trigonal planar configuration is typical of sp^2, which form σ bonds. The pure *p* orbital forms a π bond. Finally, sp^3 lobes are oriented towards the vertexes of a regular tetrahedron. In this case, all the four orbitals are hybridised and form σ bonds.

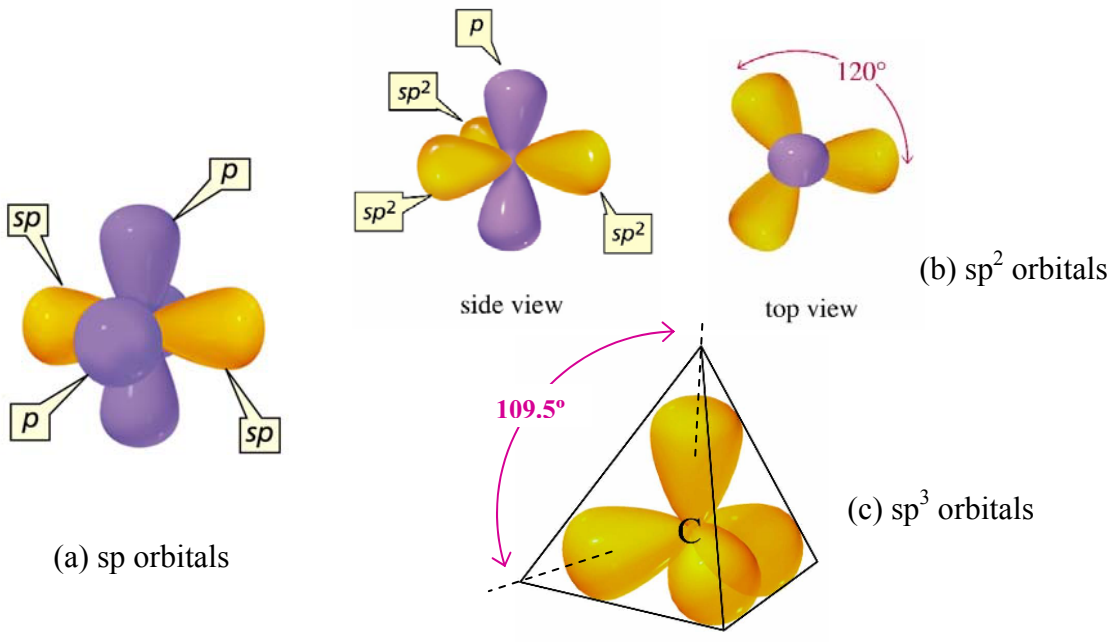

Figure 2.5: Spatial arrangement of orbitals in carbon atom in the case of (a) *sp*, (b) sp^2 and (c) sp^3 hybridisations.

Carbon presents allotropy, i.e. three different phases have been found in solid state: graphite, diamond and amorphous carbon. They are constituted by carbon atoms bonded by sp^2, sp^3 and combinations of both hybridisations, respectively. There exists another configuration of carbon: the polymer-like form. It is found when carbon is diluted with hydrogen, and it presents low hardness, high transparency and electrically it behaves as an electric insulator. The spatial distribution of polymeric carbon comprises a rich variety of shapes and lengths, which gives rise to compounds with different chain types. They are divided into open (aliphatic) and closed, being the former lineal or ramified and the latter alicyclic or aromatic.

· Graphite

Graphite shows a stable trigonally bonded crystal structure (figure 2.6). Carbon atoms become bonded by σ bonds due to three superposed sp^2 orbitals, adding a π bond that results from the interaction of pure *p* orbitals. This material is soft, optically opaque, chemically active, and is a good electric conductor. The atoms are organised in parallel and single-atom planes, which are called graphenes. Carbon atoms from adjacent planes are bonded by weak dispersion van der Waals forces, which allow two graphenes to slip one on each other and confers special lubricating properties to graphite. The in-plane bond length is 0.142 nm, whereas the inter-plane distance is 0.341 nm. Graphite crystallizes in hexagonal close-packed (h.c.p.) network, and its most important applications are pencil tips, electrodes and solid lubricants.

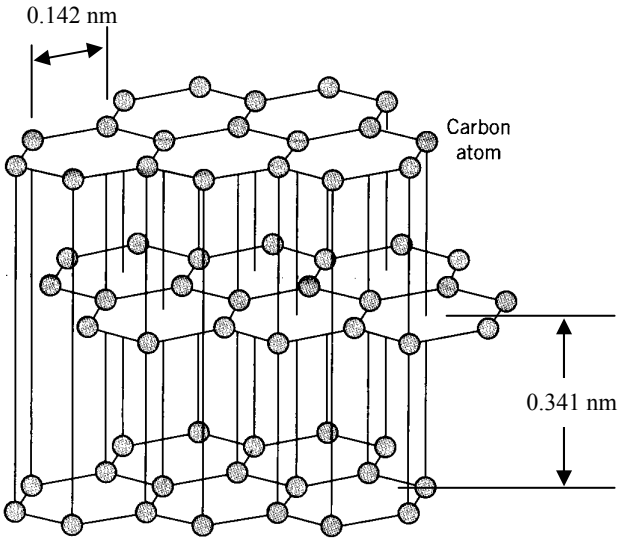

Figure 2.6: Crystalline structure of graphite, showing a portion of three graphenes.

· Fullerenes and nanotubes

Buckminster fullerenes were introduced in 1980s as an additional form of carbon. They were formulated as C_{60}, and consist on spherical lattices formed by 60 sp^2-bonded carbons (figure 2.7.a). Extensive research on fullerenes has been undertaken for medical applications using fullerenes as substitutive ligands or in biosensor devices. In the early 1990s, a subset of fullerene science appeared. The preparation of new cylindrical structures

called carbon nanotubes was firstly reported by Ijima [1991]. They were called multi-walled nanotubes, since they consisted on multiple graphenes that formed a cylinder surface (figure 2.7.b). Further refinements permitted the deposition of single-wall nanotubes. Both fullerenes and nanotubes were initially grown by arc discharge and laser ablation techniques, and recently they have been produced by CVD method. Most carbon nanotubes applications include field emission devices, fuel cells, cold cathodes and ultrahigh-strength structural materials.

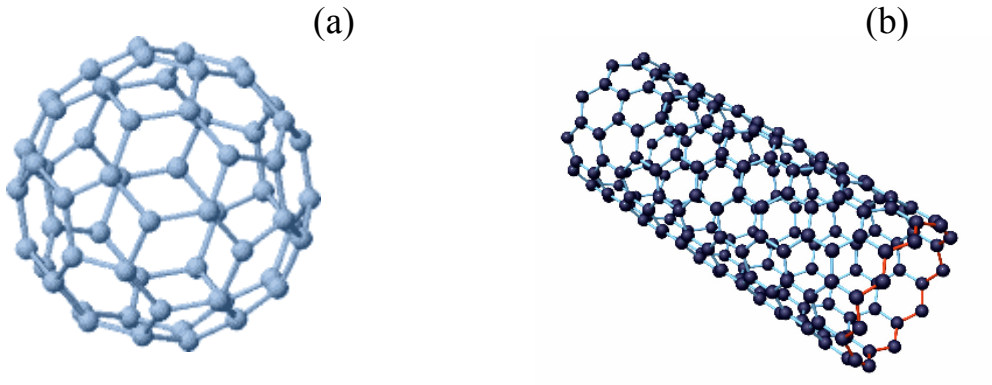

Figure 2.7: (a) fullerene C_{60} and (b) nanotube as examples of carbon nanostructures.

· Diamond

Diamond structure results from the metastable tetragonal (σ) bonding of carbon atoms, and is only stable at high pressure and high temperature. It is considered to be a material with various extreme physical properties. First of all, it exhibits the highest elasticity module known to date. In fact, diamond establishes the ultimate hardness limit basically due to the superior strength of its chemical bonds. Complete sp^3 hybridisation occurs and, therefore, all atoms become bonded via strong frontal σ bonds. The C-C bond (sp^3) is 0.154 nm long, a bit longer and weaker than that in graphite (sp^2), and its crystallographic structure consists of two superimposed face-centred cubic (f.c.c.) lattices shifted by one-quarter of the cube diagonal (figure 2.8). Such bonds confer the extreme hardness of diamond, and the highest atom density among all solids.

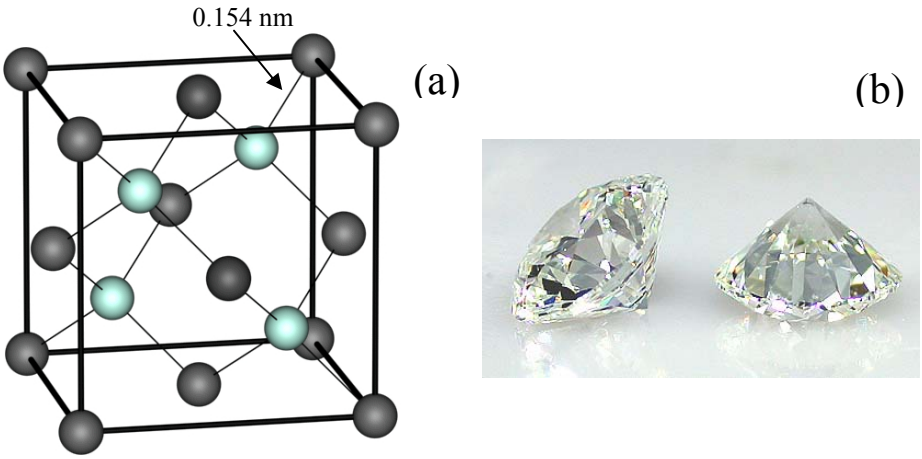

Figure 2.8: (a) Schematic picture of a diamond lattice and (b) examples of cut diamond gemstones

Polymeric carbon can also host a great fraction of sp^3 bonds, although the majority of them come from C-H groups and therefore the material is soft. Diamond is mostly employed in cutting tools (edges), abrasive coatings (dust) and jewellery. A prominent use of diamond in electronic applications has taken place due to the interesting properties when the material is chemically doped, especially with the recently discovered superconductivity [Ekimov E.A., 2004]. Table 2.1 provides a list of some applications of diamond along with the required properties.

APPLICATION	**Required properties**
Ultrahard tool coatings	High hardness
Abrasive grain	High hardness
Sunglass lenses	High hardness, scratch resistance, optical transparency
Computer hard disk coatings	High hardness, low wear
Watch cases	High hardness, scratch resistance
Prosthetic coatings	High hardness, low wear
Optical coatings	High refractive index
Infrared laser windows	Transparency to IR
Semiconductor devices	Large bandgap
Semiconductor device heat sinks	High thermal conductivity

Table 2.1: List of some applications of diamond and the required properties.

Diamond conventional preparation requires high-pressure and high-temperature processes (HPHT). Nowadays, thin films of single crystal diamonds in thin film form are prepared by CVD method at high deposition rates, which opens new perspectives for the diamond applications.

2.1.2. Amorphous carbon

Besides diamond and graphite, carbon can form an amorphous phase, which is the nucleus of this thesis. Amorphous carbon (a-C) is obtained under controlled deposition of the amount of diamond, graphite and polymeric phases. Its close relationship with DLC is analysed next by citing some key definitions from the International Union of Pure and Applied Chemistry (IUPAC).

Diamond-like carbon:
"Diamond-like carbon (DLC) films are hard, amorphous films with a significant fraction of sp^3-hybridized carbon atoms and which can contain a significant amount of hydrogen. Depending on the deposition conditions, these films can be fully amorphous or contain diamond crystallites. These materials are not called diamond unless a full three-dimensional crystalline lattice of diamond is proven."

Amorphous carbon:
"A carbon material without long-range crystalline order. Short range order exists, but with deviations of the interatomic distances and/or interbonding angles with respect to the graphite lattice as well as to the diamond lattice."

Actually, the IUPAC has considered that *hard amorphous carbon films* and *diamond-like carbon films* are synonym expressions. In our case, the prepared a-C films have high hardness values and other important properties very close to diamond. From the structural point of view, the short order up to 6-10 atomic distances is synonymous of systems with nanocrystalline structure. Thus, this material will be called DLC from now onwards in this thesis.

The DLC matrix does not contain only one determined hybridisation, but contains all three in different proportions. A phase diagram of carbon as a function of sp^2 and sp^3 bonding, and of hydrogen content, is shown in figure 2.9. It presents a ternary diagram, where amorphous carbon is understood to be a mixture of the three "pure" phases. There, a-C showing disordered graphitic structure lies in the lower left hand corner, and hydrocarbon polymers are located next to the hydrogen abundant region, where films cannot be deposited. Preparation of a-C containing large sp^3/sp^2 ratio is desirable to obtain "diamond-like" properties. In this way, sputtering and PECVD increase sp^3 bonding, although the latter technique provides H-rich samples. High plasma density PECVD reactors are necessary to maximise sp^3 bonding and simultaneously diminish hydrogen content. When the sp^3 fraction reaches a high degree, a-C is denoted as tetrahedral a-C (ta-C) because tetrahedral bonding due to this hybridisation is predominant [McKenzie D.R., 1996]. The gaps defined between the different phases comprise alloys with intermediate properties.

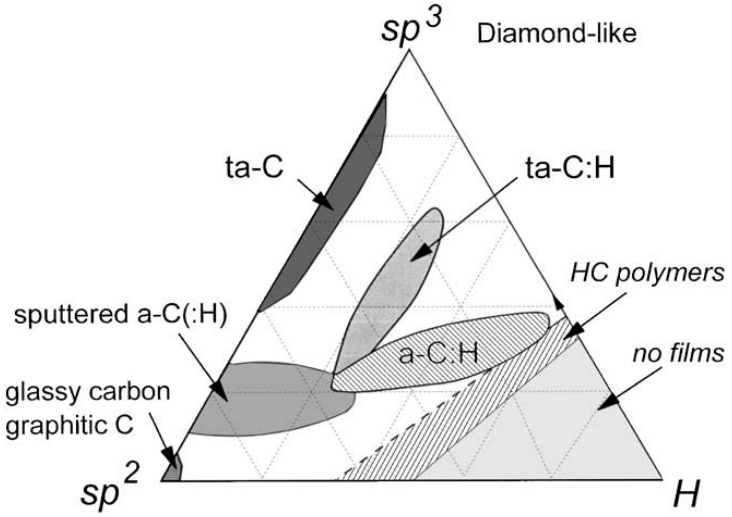

Figure 2.9: Ternary phase diagram of carbon alloys, as a function of hybridisation type [Ferrari A.C., 2000].

We can imagine the microstructure as a system of covalently bonded carbon atoms organised in a 3-D network, containing a random distribution of sp^2 and sp^3 bonds (figure 2.10). This ensures a rich variety of a-C microstructures and properties, and then a classification in sub-categories with common microstructures as presented in figure 2.9 is preferred. The high-range correlation disappears by the effect of such spatial randomness and the network becomes globally disordered. Nevertheless, an intermediate range order on the nanometer scale has been found.

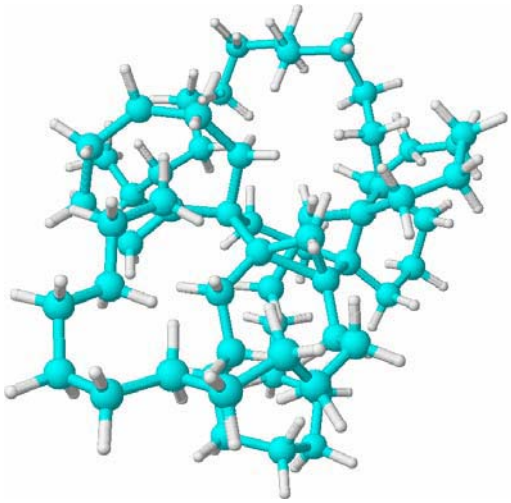

Figure 2.10: Molecular schematic of high-density amorphous carbon network.

The key parameters to define the disordered structure of DLC are sp^3 fraction, hydrogen content and, in a second term, clustering of sp^2 phase, which takes special relevance in the electronic properties of this material. Nuclear Magnetic Resonance (NMR) and Electron Energy Loss Spectroscopy (EELS) are the most common characterization techniques to derive the sp^3 fraction [Robertson J., 2002]. Mass density is evaluated through X-Ray Reflectivity (XRR) technique and shows a correlation with sp^3 amount. However, the presence of hydrogen complicates this analysis since CH_x groups are sp^3 bonded and contribute to a decrease in material density. Raman spectroscopy takes advantage of vibrational properties of the DLC network to determine its sp^3 fraction, and supposes one of the most used methods for this task. Fourier Transform Infrared spectroscopy (FTIR) and X-Ray Photoelectron Spectroscopy (XPS) constitute other important tools to study the composition (H content) and bonding structure of DLC.

A statistical description of atom distribution in DLC random network is yielded by the radial distribution function (RDF). It is defined as the probability of finding an atom at a given distance from a given atom. The reduced RDF, *G(r)*, can be derived from diffraction experiments data:

$$G(r) = \int_0^\infty k[S(k)-1]\sin(kr)dk \qquad (2.1)$$

where k is the wave-number and *S(k)* is the structure factor, which is defined by equation 4.3 (chapter 4). At the molecular scale, the RDF consists in a series of peaks defined by each shell of neighbouring atoms. This provides a 1-D representation of the network

structure. Hence, the first peak is due to the first bonded neighbours and gives the bond length r_1. The area under this peak provides the corresponding coordination number, N_1. The second neighbours at distance r_2 form the second peak, whose area provides N_2, and so on. Another relevant structural parameter is the bond angle, θ, given by:

$$r_2 = 2r_1 \sin\left(\frac{\theta}{2}\right) \tag{2.2}$$

The zoom of the simulated network in figure 2.11 shows the physical meaning of these structural variables.

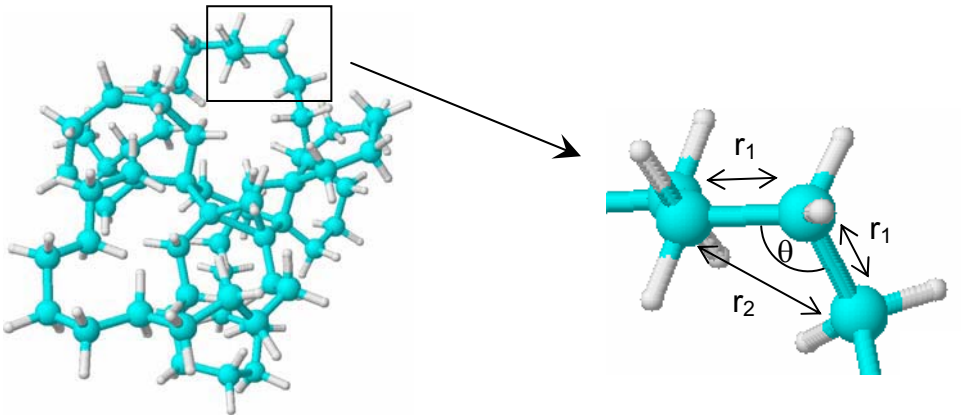

Figure 2.11: Identification of structural parameters in DLC network.

Table 2.2 shows a comparison of N_1, N_2, r_1, r_2 and mass densities for different forms of carbon. These parameters give a rough idea of the structure of any a-C. For instance, the similar values of r_1, N_1 and density for diamond and ta-C evidence the high sp^3 content in the latter. However, RDF peaks of ta-C are relatively wide and N_2 differs considerably from that of diamond, which indicates large disorder and the existence of sp^2 bonds.

Material	**r_1 (nm)**	**N_1**	**r_2 (nm)**	**N_2**	**Density (g/cm^3)**
Diamond	0.154	4	0.2512	12	3.515
Graphite	0.142	3	0.245	6	2.267
Glassy C	0.1425	2.99	0.245	6.1	1.49
a-C (evap)	0.143	3.3	0.253	8.8	2.0
a-C (sput)	0.146	3.34	0.249	6.7	2.44
ta-C	0.152	3.9	0.248	7.66	3.2

Table 2.2: Structure parameters for various forms of carbon: bond length (r_1), first coordination number (N_1), second neighbours distance (r_2), average number of second neighbours (N_2), and mass density.

Besides its attractive mechanical properties, DLC is a semiconductor at room temperature that shows remarkable surface and optical properties. These features are strongly dependent of its structure, namely of the sp^3/sp^2 ratio and the hydrogen content. It is considered a chemically and thermally stable material, although it shows significant loss of hydrogen and CH_x groups when heated around 400ºC and above. Its structure can also be modified under UV or ion beam irradiation. Table 2.3 summarizes some important physical parameters of carbon compounds, either amorphous or crystalline, including graphite and diamond allotropic forms.

Material	Density (g/cm^3)	Optical bandgap (eV)	Hardness (GPa)	sp^3 (%)	H (%)
Diamond	3.515	5.5	100	100	0
Graphite	2.267	0	-	0	0
Polyethylene	0.92	6.0	0.01	100	67
C_{60}	-	1.6	-	0	0
Glassy carbon	1.3-1.55	0.01	3	0	0
Evaporated C	1.9	0.4-0.7	3	0	0
Sputtered C	2.2	0.5	10	5	0
ta-C	3.1	2.5	80	80-88	0
Hard a-C:H	1.6-2.2	1.1-1.7	10-20	40	30-40
Soft a-C:H	1.2-1.6	1.7-4.0	<10	60	40-50
ta-C:H	2.4	2.0-2.5	50	70	30

Table 2.3: Basic properties of diamond, graphite, C_{60} and polyethylene compared to different amorphous carbons [Robertson, J., 2002].

The density of states (DOS) of carbon as a function of energy, *N(E)*, displayed in figure 2.12, can be explained in terms of the formed bonds. The σ bonds of all carbon sites and the C-H bonds form occupied σ-states in the valence band and empty σ^*-states in the conduction band. These states are separated by a wide σ-σ^* gap. Parallel to the σ-states, filled π-states and empty π^* states are formed close to the Fermi level by the π bonds of sp^2 and *sp* sites. Here, the π-π^* gap is much narrower than that of σ-σ^*.

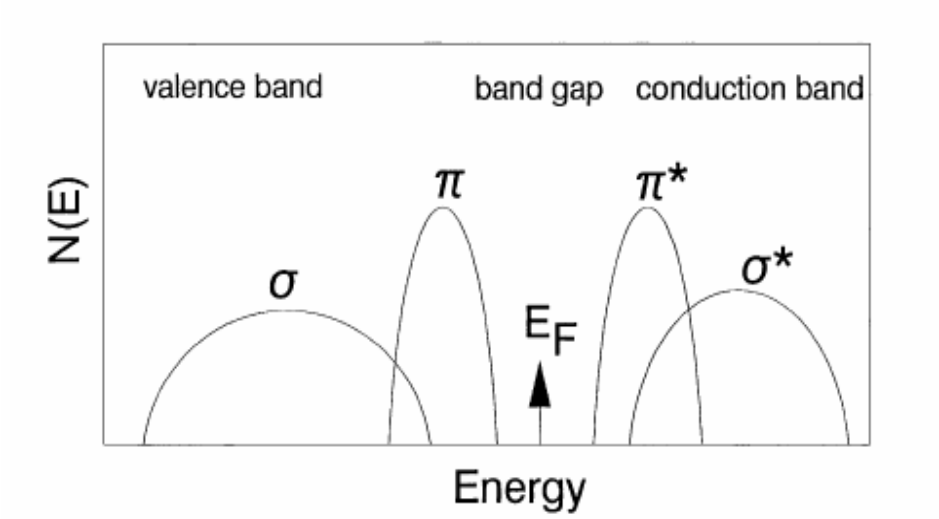

Figure 2.12: Schematic DOS of carbon showing σ and π states.

Due to the DOS configuration, the arrangement of sp^2 sites is a crucial factor for the electronic properties and the optical gap of amorphous carbon. The optical gap depends mainly on the sp^2 fraction in DLC, and it decreases as this fraction increases. Such gap is also strongly dependent on clustering and orientation of sp^2 states. According to the cluster model [Robertson J., 1986], the sp^2 sites are embedded in a sp^3-bonded matrix, which controls the mechanical properties. The Huckel approximation permits a simple description of electronic structure and bonding of a-C through this model. In it, σ and π states are treated separately because they lie at different energies and they show a weak interaction due to their respective orthogonal orientation.

Regarding the outstanding mechanical properties of DLC, both hardness and elastic modulus reach high values, and can be tailored by controlling the sp^3 fraction. Although hardness of DLC ranges from 10 to 30 GPa, the rigid network of the films shows an intrinsic compressive stress ranging from 0.5 to 7 GPa. This high stress supposes an important drawback in the production of DLC coatings, since it limits the film thickness to less than 1 μm. In fact, the accumulation of micro-strains within the amorphous matrix leads to a global compressive stress that is large enough to damage the film through the development of cracks and strains that difficult the adhesion to substrate. DLC films thicker than 50 nm are generally so stressed that they lose their consistency and delaminate.

Stress relaxation is possible through doping with N, Si or metals, as well as by post-annealing or incorporation of nanometric particles (DLC nanocomposites) [Zhang P., 2002] [Chen L.Y., 2003]. But these operations generally reduce hardness and elastic modulus. Metal incorporation in a DLC matrix has been proved to reduce stress below 1 GPa and maintain hardness and wear rate with acceptable values [Dimigen H., 1987]. As commented in chapter 1 and discussed in chapter 8, this improvement is related to the special structures of Me-DLC films conferred by each metal.

Low stress values are also achieved by depositing alternated hard and soft a-C layers (a-C hard / a-C soft) [Ager J.W., 1997] [Logothetidis S., 2000]. The resulting multilayered structure shows a lower overall stress, and hardness is almost unaffected. Metal and a-C multilayers (Me/a-C) [Bertran E., 2003], as well as a-CN/a-C structures [Pino F.J., 2001], were also deposited with similar results. Bias-graded deposition of DLC provides the best tribological performance through surfaces showing high sp^3/sp^2 ratios, which gradually decrease from the surface to the interface in order to enhance adhesion [Zhang S., 2004]. Another way to improve coating adhesion consists in growing a buffer layer (Ti, Cr) prior to DLC deposition. All the structures commented above are represented in figure 2.13.

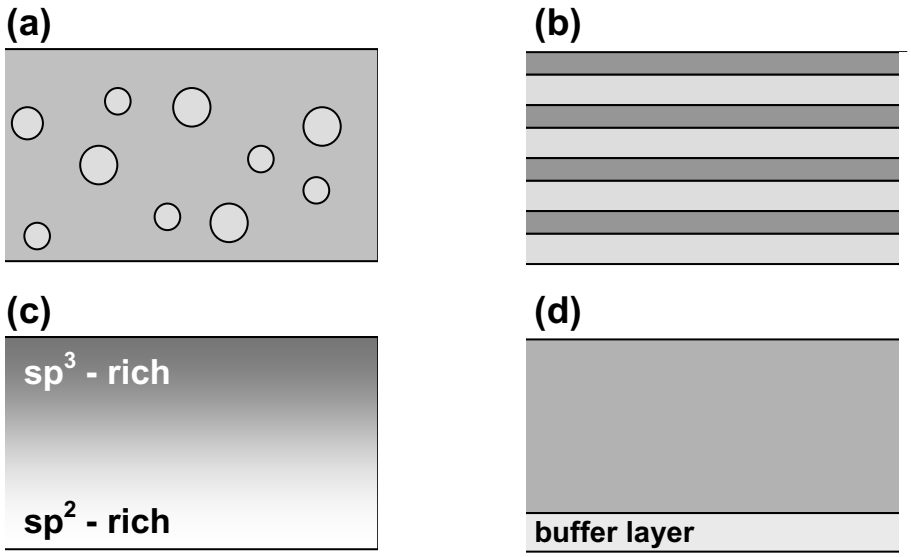

Figure 2.13: DLC structures (cross-section) that present low intrinsic stress are (a) nanocomposites, (b) multilayers, (c) bias-graded films and (d) coatings on buffer layers.

DLC films with hydrogen are mostly exploited in tribological applications due to their low friction coefficient and low wear rate. In all environments, the tribological behaviour of DLC is controlled by an interfacial transfer layer formed during friction [Voevodin A.A.,

1996b]. It consists of a friction-induced sp^2-rich layer formed on the surface of the counterpart, which is produced by the micro-debris coming from an initial abrasion stage and shows an effective lubricating effect. The low shear strength of this transfer layer material provides a friction coefficient down to 0.05, reaching values even lower than 0.01 when measured at high vacuum. Thus, DLC presents a valuable use as lubricant for applications where liquid lubricants are not convenient.

Besides wear and corrosion resistant, DLC is also known to be a highly hydrophobic material. The C-H groups located on the film surface diminish the wettability, which is parameterised by the contact angle held between a water drop and the film surface (chapter 4). DLC exhibits typically a contact angle of 55-70º, although it can be increased by adding metals such as Fe or Al. In the case of Al-DLC films, the contact angle exceeds 100º [Chen J.S., 2001].

Low roughness is another surface property that makes DLC films suitable for their application as protective coatings. DLC layers show a flat and smooth surface, with their roughness being minimised when deposited by arc evaporation. Measurements carried out by AFM provided values of RMS surface roughness below 0.05 nm for DLC either deposited by sputtering or PECVD [Peng X.L., 2001]. This means that statistically no more than one atom overlays the “average” flat surface, improving thus the tribological properties. Moreover, surface roughness of ultra-thin DLC films is revealed to follow fractal scaling laws, i.e. it is related to film thickness through an exponential function [Casiraghi C, 2004].

2.2. Thin film synthesis

DLC can only be obtained at conditions far away from equilibrium, and so it is not spontaneously found in nature. The control of the growth parameters broadens the field of carbon microstructures and, in parallel, the properties of this material. Despite the absence of a crystalline structure, DLC shows mechanical properties similar to diamond. This fact, in conjunction with the relatively lower cost of production and the great variety of growth techniques, makes this material attractive for technology and industry because of its innumerable applications.

2.2.1. Growth mechanism

In order to produce a-C films with diamond-like properties, i.e. DLC films, it is necessary to maximise the C-C sp^3 bonding, which is the responsible of the mechanical properties of this material. The key parameter that provides sp^3-rich DLC films is the ion bombardment energy during deposition [McKenzie D.R., 1996] [Pharr G.M., 1996]. C^+ ion energies of around 100 eV are needed to achieve highest sp^3/sp^2 ratios.

Preferential sputtering of sp^2 sites during DLC film growth was considered as the main mechanism that increased sp^3 content [Spencer E.G., 1976]. Later, Lifshitz et al. [1990] observed that DLC film growth was sub-surface. The so called *subplantation model* considers the progressive densification of DLC in a sub-surface layer, which is associated to the formation of metastable sp^3 sites owing to the penetration of energetic ions. The penetration threshold, E_p, can be approximated to:

$$E_P \approx E_d - E_B \tag{2.3}$$

and it depends on the displacement threshold, E_d, namely the minimum energy for an incident ion to displace an atom from a bonded site, generating a permanent vacancy-interstitial pair. It is influenced also by the surface binding energy, E_B, which is the sublimation or cohesive energy for C ($E_B \approx 7.4$ eV).

Incoming neutrals and low-energy ions do not penetrate the surface, but may stick onto the film surface, generating there a sp^2 rich outer layer. Moreover, the surface population is increased by subplanted high-energy ions that overcome an energy barrier and, then, are

able to relax to the more stable surface sp^2 states by an energy dissipation process through a thermal spike.

The penetration fraction, f, corresponding to incoming ions with an energy E higher than E_P is approximated by [Robertson J., 2002]:

$$f = 1 - \exp\left(-\frac{E - E_P}{E_S}\right) \tag{2.4}$$

where E_S is a constant. Taking into account this penetration probability, the density of the subplanted layer in ta-C exceeds that of graphite with the following ratio:

$$\frac{\Delta\rho}{\rho} = \frac{f\phi}{1 - f\phi + \beta} \tag{2.5}$$

Here, ρ is defined as the density of sp^2-carbon, $\Delta\rho$ is the density increase, ϕ is the fraction of energetic ions with energy E_i, and β is the relaxation rate in the thermal spike:

$$\beta \approx 0.016\left(\frac{E_i}{E_0}\right)^{5/3} \tag{2.6}$$

in which E_i is the ion energy, and E_0 is the diffusion activation energy. Figure 2.14 schematizes the basic processes in this two-state model. Recently, a new model has also accounted for a third state, corresponding to interstitial sites with high energy [Robertson J., 2005]. This results in a small perturbation of equation 2.5.

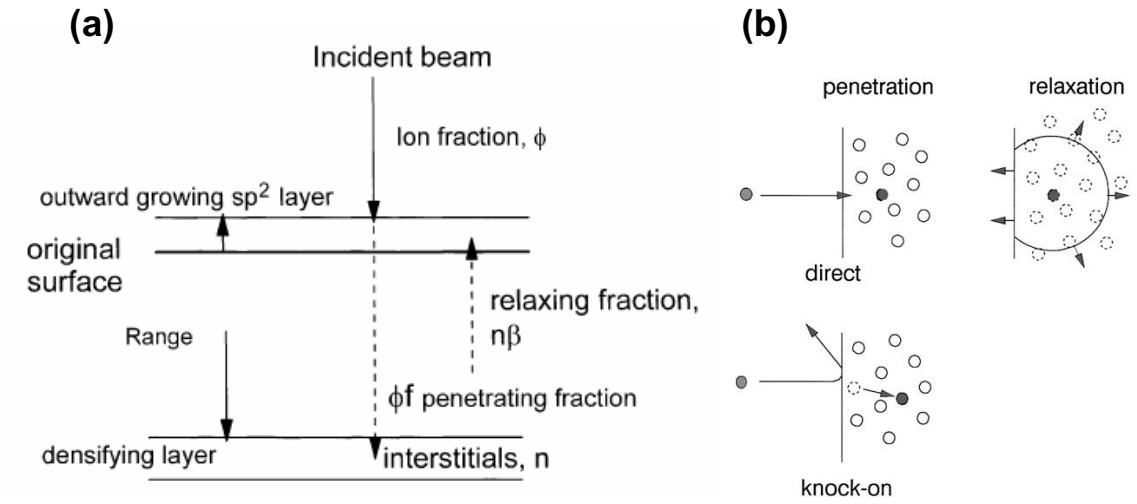

Figure 2.14: (a) Diagram of the subplantation process and (b) basic processes in subplantation model [Robertson J., 2002].

In the subplantation model, incident ions can penetrate in two ways: either directly or indirectly by knock-on process. The relaxation of a densified region drives atoms from sp^3 to sp^2 sites through a thermal spike, with these processes presenting time scales of 10^{-12} and 10^{-9} s, respectively. The thermal energy coming from incident ions diffuses outwards by means of an expanding front, which shows the following temperature profile [Seitz F., 1956]:

$$T(r,t) = \frac{Q}{c(4\pi Dt)^{3/2}} \exp\left(-\frac{r^2}{4Dt}\right) \tag{2.6}$$

where r is the distance from the impact, t is the time from the impact, D is the thermal diffusivity, c is the thermal capacity and Q equals E_i minus the energy lost in displacements.

Next in this section we highlight the importance of controlling the bias voltage applied to the substrate in order to control the DLC microstructure, which in turn affects mechanical, optical and electric properties [Staryga E., 2005]. As long as ion energy is limited by the substrate biasing, the sp^3 content is modulated by the supplied power to the cathode-holder. Fallon et al. [1993] obtained a sp^3 fraction dependence from ion energy in which maximum of this fraction was 80% between 100 and 200 eV. On the other hand, figure 2.15 shows the curve of sp^3 fraction as a function of bias voltage for ta-C deposited by FCVA method in more recent experiments [Polo M.C., 2000]. In these, the sp^3 content varies from 84 to 88% in a bias voltage window from -20 to -350 V. The correlation between this small variation of sp^3 content and mass density though bias voltage is shown in figure 2.16. However, more results also plotted in figure 2.16 indicate that compressive stress is correlated with bias voltage, whereas no apparent relationship between sp^3 fraction and stress has been observed.

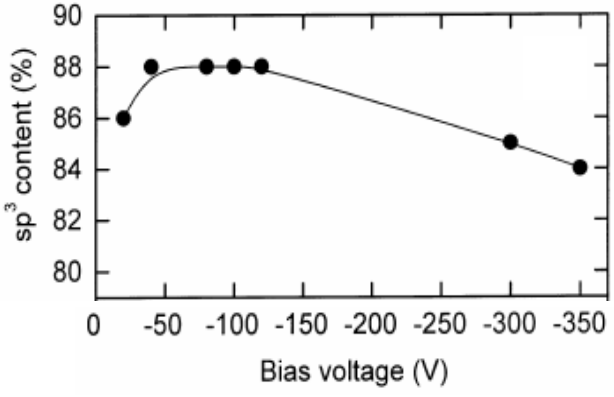

Figure 2.15: Dependence of sp^3 content on bias voltage of ta-C films [Polo M.C., 2000].

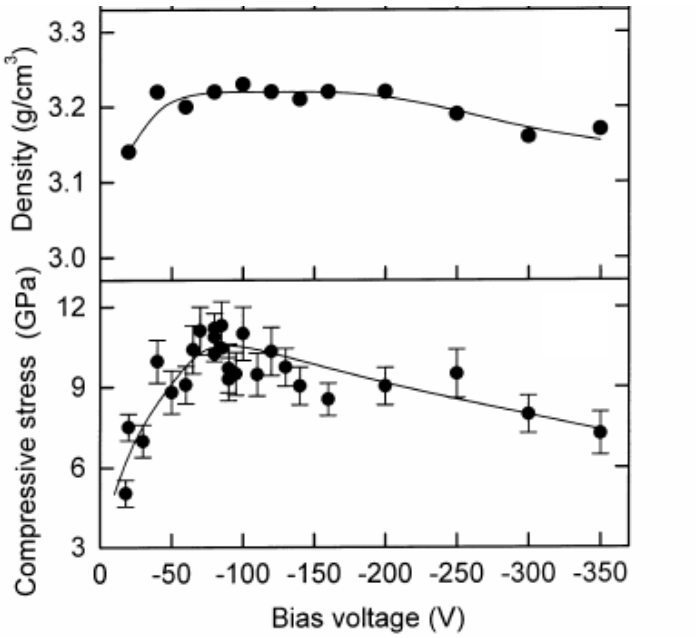

Figure 2.16: Dependences of mass density and compressive stress on bias voltage of ta-C films [Polo M.C., 2000].

Ion energy adopts once more a critical role in the deposition of a-C:H films. However, the ion fraction is typically 10% of the total flux, in contrast with the total ionisation in arc discharges used in the production of ta-C films. As shown in chapter 5, a-C:H films can be deposited from different precursors: CH_4, C_2H_2, C_2H_4, and C_6H_6, being the former gas employed in this thesis. The subplantation model is still valid in this context, since one essential issue is the penetration of carbon and hydrocarbon ions across the surface layer. Molecular reactions in the plasma and dehydrogenation of the layer during deposition are additional topics to be considered in a-C:H films growth. The case of DLC preparation from CH_4 glow discharge is treated in chapter 5.

DLC deposition must be performed at room temperature in order to favour the amorphous state. Substrate heating is a thermal mechanism that yields extra energy to the impinging species that come from the plasma. Deposited atoms use this thermal energy to diffuse on the surface until they reach equilibrium sites. Thus, high temperature processes lead to ordered, crystalline samples. A disordered network is achieved when species are frozen as soon as they impact on the depositing surface, and so substrate cooling is necessary. However, the elevated toughness acquired by DLC films has detrimental effects on film consistency. As mentioned in section 2.1.2, these films are highly stressed. This effect

comes mainly from the low temperature of the substrate, which confers the non-equilibrium conditions to the process. Incoming species from the plasma get fixed in their impinging sites, and therefore the potential energy acquired by the DLC matrix increases its stress.

2.2.2. Deposition techniques

The production of a-C thin films is carried out by a large variety of deposition techniques, some of them adequate for laboratory studies while some others are preferred in industrial production. Since contamination of the grown layers must be minimised, all the preparation processes require low base pressures. The different methods to deposit DLC exhibit also three characteristics [Silva S.R.P., 2003]:

(*i*) A plasma is used as the source of reactive species.
(*ii*) The substrate is found, in general, around room temperature. At least there is not need to maintain a high substrate temperature during the process as in classical CVD processes.
(*iii*) Energetic particles (ions and/or neutrals) participate in the deposition process.

· Ion beam deposition

Ion beam deposition was the first method used for the synthesis of DLC [Aisenberg S., 1971]. Carbon and hydrocarbon ions coming from a graphite cathode are condensed in an energetic beam and produce sp^3 states as they impinge on the growing film. Ion beam sources operate efficiently within an ion energy range of 100-1000 eV. Mass selected ion beam (MSIB) techniques are addressed to obtain ion beams with ion species of a determined energy. Ions pass through a magnetic filter that selects charged species with a fixed e/m ratio, being e the electric charge and m the ion mass. Unfortunately, the ion beam is weakly ionised and, thus, mechanical properties of DLC are not optimal.

· Sputtering

Sputtering is the most used technique in industrial environment. The impinging species are commonly sputtered from a graphite target, which is RF or DC powered, in an Ar glow discharge. A magnetron is usually placed behind the target in order to enhance the sputtering rate by increasing the ionisation degree in the plasma. The energy of the ion

species being deposited is modulated by applying a DC bias to the substrate, and by employing a magnetron whose magnetic field reaches the substrate surface (unbalanced magnetron). Figure 2.17 shows a typical equipment setup for sputtering deposition.

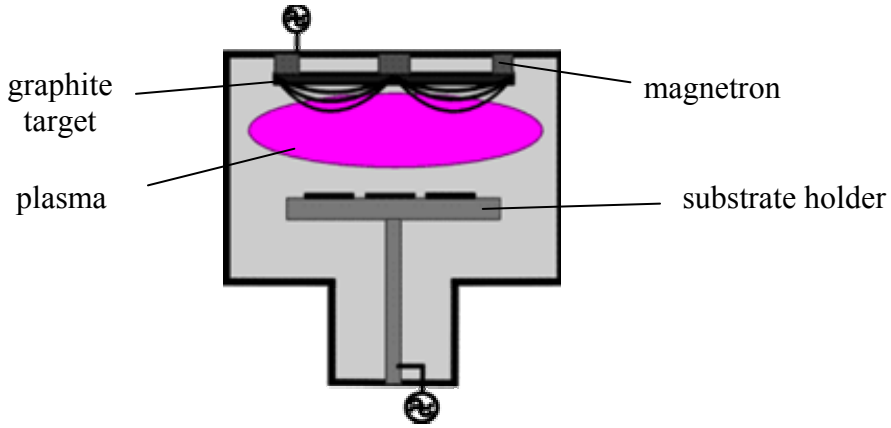

Figure 2.17: Schematic of experimental setup for deposition by AC magnetron sputtering.

Reactive sputtering process is also possible if hydrogen or hydrocarbon source gases are added to Ar. An alternative sputtering process can be performed without plasma: an Ar ion beam from an ion gun sputters a carbon target, say graphite, and another beam bombards the growing film to promote sp^3 formation. This method is called ion beam assisted deposition (IBAD). Like in the ion beam process, sputtering provides poorly-ionised flows of particles.

. Cathodic arc

Cathodic arc constitutes one of the oldest vacuum deposition techniques [Sanders D.M., 2000]. The arc discharge is concentrated at the cathode surface, where high ion densities ($\sim 10^{12}$ A/m^2) form non-stationary spots. The ionisation of species reach 100% of the total flux, and the maximised parameter is the electron current to the anode, which is called arc current. The ion current is about 10-100 times less than the arc current. This method is really appropriated to obtain hard DLC films, with a significant sp^3 fraction, but certain problems have limited its use in laboratories worldwide. First of all, films may present serious inhomogeneities due to the instabilities caused by the location of the arcs in the cathode, which also is the substrate holder. Secondly, the generation of macroparticles requires the installation of a filtering device. Filtered cathodic vacuum arc (FCVA) solves

the last problem by means of a magnetic filter, either in single bend or S-bend configuration [Robertson J., 2002].

· Pulsed laser deposition

Pulsed laser deposition (PLD) provides energetic ions, as in cathodic arc processes. Therefore, it is possible to deposit DLC films with high sp^3 content by this technique, without the necessity of substrate biasing or great current discharges [Voevodin A.A., 1996a]. The intense energy pulses (15-30 ns) of a laser beam are able to vaporise a carbon target, which shows major advantages when it is graphite due to minimisation of droplets emission. Fluxes of neutrals, ions and particulates are ejected from the target through an intense plasma, which is termed plasma plume. The first PLD depositions were performed by means of Nd:YAG lasers, operating at the 1064 nm wavelength. Nowadays, excimer lasers are the preferred ones because higher-quality DLC is obtained using shorter wavelengths, for instance 193 and 248 nm (ArF and KrF lasers, respectively). The structures of DLC samples grown by PLD can be nanocrystalline diamond and ta-C.

· Plasma-enhanced CVD

Plasma-enhanced CVD (PECVD) is a very popular technique of depositing DLC films. Plasma in a reactor is ignited between two electrodes with different areas, A_1 and A_2, giving place to an asymmetrical discharge. The supplied power cannot be DC, since DLC is electrically insulating. Thus, these PECVD processes employ capacitively coupled RF power or pulsed-DC power. As depicted in figure 2.18, power is driven to the small electrode (cathode), where the substrate is placed, and the reactor walls are usually grounded (anode).

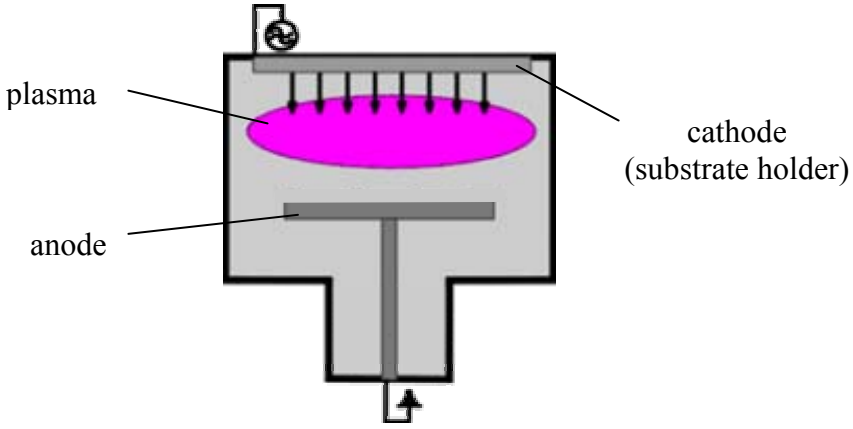

Figure 2.18: Layout of a PECVD reactor.

The negative bias of substrate cathode accelerates the bombarding ions to create sp^3 sites. However, the enhancement of ion-to-neutrals rate in the discharge needs low-pressure plasmas, but very low pressures avoid self-maintained discharge regime. This requirement is accomplished by raising the supplied power or by coupling an external magnetic field to the sheaths. The latter is performed in inductively coupled plasmas (ICP). Electron cyclotron resonance systems (ECR) use both microwaves and magnetic field for a resonant transfer of energy to the electrons in the plasma.

· Electron cyclotron wave resonance (ECWR)

When trying to couple electromagnetic radiation to a plasma, this behaves as a conductive medium and absorbs totally the incident waves within a characteristic absorption depth or "skin" depth. The plasma becomes transparent to the electromagnetic waves only when the excitation frequency exceeds the plasma frequency. However, RF excitation frequencies require very low plasma densities. A more efficient method is based on reducing the plasma conductivity by applying a magnetic field (~ 20 G) to the system. The setup of this technique is shown in figure 2.19.

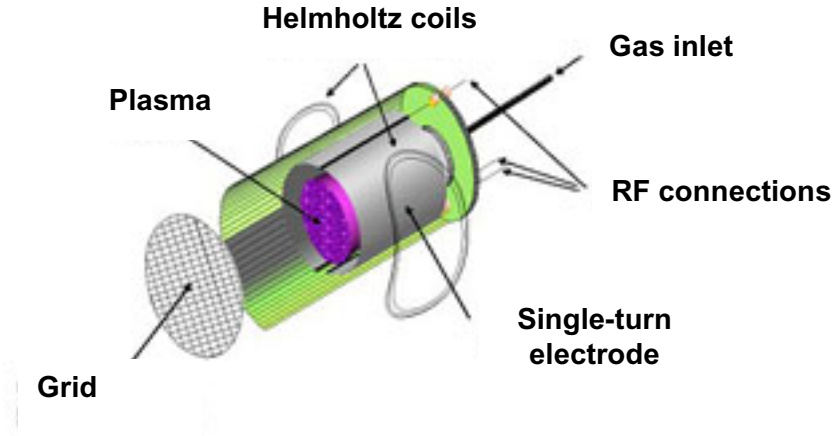

Figure 2.19: Schematic of an ECWR plasma beam source.

Since the electrons are confined in cyclotron orbits around the field lines, conductivity is inhibited. Hence, the electromagnetic radiation can propagate and can be absorbed across the plasma, which contributes to increase the plasma density and generates the propagating electromagnetic modes [Rodil S.E., 2000]. One of these modes matches the dimensions of the plasma chamber, being thus responsible of the resonance effect.

2.3. Applications

The great variety of applications of DLC is mainly addressed to hard coatings with special tribological properties. It is also true that these properties can be tuned by modifying DLC structure and by incorporating other elements [Hauert R., 2000], whereas other properties ensure its performance as optical filter or as components with electronic functionality.

2.3.1. Industrial machinery and tools

The fastest growing market for DLC application is the automotive industry, in which DLC, ta-C, W-DLC and WC/C multilayers are being preferentially developed as hard and tribological coatings [Hauert R., 2004]. Automotive industry demands solutions for preparing low friction and wear resistant coatings for lubricant performance on components. DLC fulfils these requirements and has been tested on a large number of automotive components: gears, wrist pins, valve filters and fuel injector parts. Figure 2.20 shows an example of some DLC coated objects.

Figure 2.20: WC/C coated spur gears from Balzers.

All these components are being coated with DLC by many coating companies. Concretely, serial production of metal-containing DLC (Me-DLC) coatings by PVD has been performed on diesel injection systems [Gåhlin R., 2001], since Me-DLC films present superior tribological properties [Grischke M., 2001] [Pei Y.T., 2005]. The modern high pressure injection systems have been developed thanks to DLC. Racing cars were the first

target in automotive applications of DLC, in order to maximise power of the motor by means of friction reduction. This issue has improved nowadays the driving conditions due to an overall reduction of gasoline consumption (Volkswagen Lupo).

The combination of elevated hardness and wear resistance of DLC is appropriated for cutting and abrasive wear instruments, like drills and other machines used in material manufacturing. Optimal frictional properties of DLC coatings increase efficiency and lifetime of ultrasonic motors (USM), which have applications in robotics and automation equipments. A highly dynamic movement is achieved when stator is coated by Si-DLC [Ko H.P., 2005]. As well as in car industry, the use of dry lubricants is indispensable for pharmaceutical and food processing systems because of requirements of chemical inertness and low friction. In this way, many machine components are protected by DLC: worm gears, lead screws, roller bearings, compressors and air bearings. Regarding textile industry, the existence of residual substances and adding compounds in yarn motivate the coating with DLC of components of textile machines in contact with yarn, as for instance spinning rings, rapiers, and needles. In injection moulding, the experts take advantage of anti-sticking properties of DLC to obtain a better product quality. The degradation of DLC when temperature exceeds 350ºC supposes an important limitation in its application on cutting tools. Some special treatments are also applied to DLC-based coatings in order to reduce the typically high compressive stress and, thus, improve adhesion of μm-thick coatings to the substrate.

Gillette Mach3 blade edges are an example of successful application of hard DLC, i.e. ta-C. These “DLC comfort edges” coated by 150 nm thick DLC appeared in 1998 and consolidated razor blades as one of the basic applications of this material.

2.3.2. Fluid storage and transport

DLC presents elevated hydrophobicity, which is a basic requirement for surfaces of fluid-contacting components and devices. DLC coatings are useful to improve surface properties of inner walls of pipes and tubes due to the reduction of fluid interaction, and suppose an excellent cladding for tools. Presently, DLC films are being considered as passivation layers for inside bottles for beverages. The inner coating of DLC films on

stainless-steel pipes (figure 2.21) is feasible by plasma-based ion immersion (PBII) applied with bipolar pulses [Miyagawa S., 2002], which supposes a great advance in coating techniques of complicated 3-D substrates (hollow-cathode). In the ambit of diffusion-barrier applications, DLC is also useful because it presents a relatively high density [Chhowalla M., 2003].

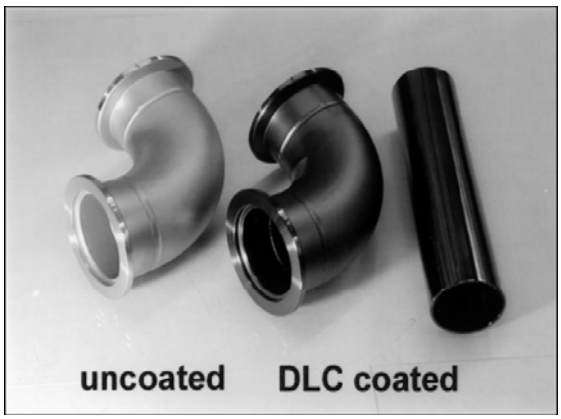

Figure 2.21: Stainless steel pipes coated by DLC films [Miyagawa, 2002].

2.3.3. Optical devices

DLC coatings are applied in the research of the new generation of optical storage devices, with the objective to protect disk and slider from head crashes. The main conditions are low wear rate and the transparency of the DLC layer in the recording wavelength. Such films should have a minimised stress and show a wide bandgap, aside of high hardness. Both parameters are tuned by sp^3/sp^2 ratio and hydrogen content, which are controlled in the deposition process. However, growth conditions should respect the integrity of polymeric substrates (low temperature). Latest research provided smooth and homogeneous DLC films, exhibiting stress values <0.5 GPa and an optical gap of 3 eV [Piazza F., 2004]. C_2H_2 as precursor gas in PECVD process provided DLC with advantageous properties for optical disk coatings [Piazza F., 2005].

The high transparency in the IR range makes DLC films suitable for surface-protection applications in IR optics [Rusli S.F., 2003]. IR antireflection coatings on Ge optics and outermost protecting layers on IR windows against rain impact damage are examples of these tasks. Regarding the operation in the visible range, sunglasses from Ray-Ban and glass plates for laser barcode scanner windows (AEGISGLASS from Morgan) show the

performance of DLC as scratch resistant coating for light transmitting surfaces [Hauert R., 2004]. The control of interferential colours suggested DLC films for their use as decorative coatings. Electroluminescence and phase-shift masks are other optical applications of DLC.

Recent investigations are addressed to solar photovoltaic applications of DLC, basically due to its semiconducting nature [Krishna K.M., 2000] and preparation cheaper than for Si-based cells. Controlling both the defects and doping of DLC structure is the current issue in this research field. As an adding remark, antireflective coatings on Si solar cells are usually DLC and nitrogenated DLC films due to their refractive index and low absorption coefficient.

2.3.4. Magnetic storage

Protection to corrosion and wear of magnetic hard disks is one of the most widespread uses of ultra-thin DLC coatings [Bhushan B., 1999a]. Without the need of light transmission, the deposited layer should be extreme smooth, continuous and chemically inert. This coating must be ultra-thin to minimise the gap between the disk and the recording head, in order to achieve great areal storage densities. Magnetic media are currently protected by an approximately 5 nm thick DLC overcoat, which consists on CN_x or a-C:H. Although the corrosion resistance of DLC fails if thickness is lower than 3 nm, ta-C films prepared by FCVA deposition show excellent corrosion and wear resistances down to 1 nm thickness, whereas atomic smoothness (0.12 nm RMS) and absence of pin-holes ensure the quality of the coating [Casiraghi C., 2004]. The head drums of video-cassette recorders are currently sputtered and PECVD-coated by DLC, to minimise degradation of signal transfer between tape heads and drums. Sony, TDK, Fuji and Panasonic sell DLC-coated data storage tapes and DVD recording tapes owing to the acceptable wear and oxidation resistance of DLC [Hauert R., 2004].

2.3.5. Electronic devices

Like diamond and CNT, DLC films have been proposed for applications involving field emission, such as field emission displays (FED). Field emission consists on electron

tunnelling through a potential barrier from a solid tip owing to the existence of an intense electric field. The field emission current density, *J*, obeys the Fowler-Nordheim equation [Schwoebel P.R., 1995]:

$$J = a\frac{(\beta F)^2}{\phi}\exp\left(-\frac{b\phi^{3/2}}{\beta F}\right) \tag{2.8}$$

where ϕ is the barrier height, F is the applied field, β is the field enhancement factor, βF is the local field at the emission site, and a and b are constants. The various forms of DLC show poor field emission properties due to the instability of the emission and the low electron site density.

Bistability of sp^2 and sp^3 phases suggests DLC to be employed in electronic switching and memory applications. In contrast to a fuse, an antifuse link is an insulating connection that switches to conducting when a current beyond a threshold is registered. The conversion of diamond-like sp^3 sites (insulating) into graphite-like sp^2 states (conducting) due to ohmic heating justifies the performance of DLC as antifuse link [Liu S., 1998]. Gerstner et al. [1998] showed that reversible conversion of sp^3 into sp^2 is possible if operating with ta-C:N, although device degradation is still a remaining issue. The outstanding tribological properties and chemical inertness of DLC are adequate for its application in microelectromechanical systems (MEMS). Since low surface roughness is essential in this case, ta-C has been studied for this application. However, this DLC form is highly stressed and must be annealed to obtain a relaxed state.

2.3.6. Biology and medicine

The right performance of biomaterials in the biological medium is shown by the re-establishment of biological and mechanical functions after their implantation into the human body [Hauert R., 2004]. The main fields of biological applications of DLC are the coating of blood-contacting implants and reduction of wear in load bearing joints. Nowadays, there is a growing interest on DLC application in orthopedic implants such as heart valves, blood pumps, stents and load bearing implants for joints (ankles, hips, shoulders). Some examples of DLC coated implants are presented in figure 2.22. In vitro tests are performed by sliding DLC coated parts against ultra high molecular weight polyethylene (UHMWPE), which simulates an organic surface.

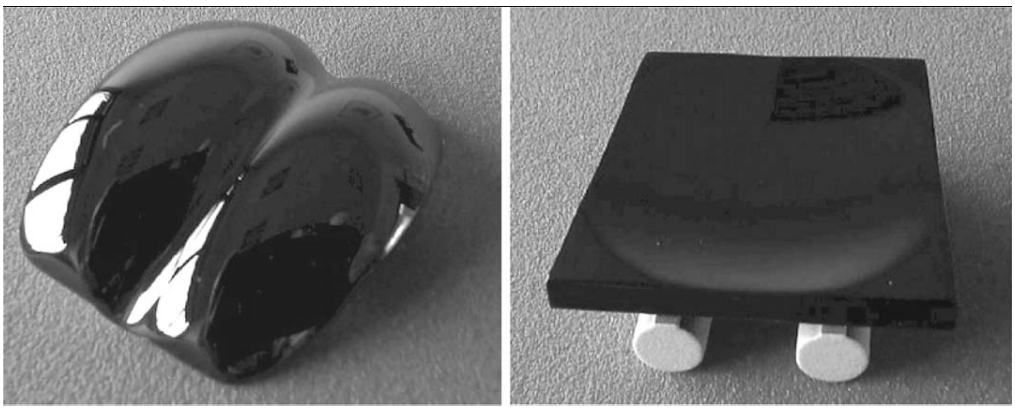

Figure 2.22: (a) Talar and (b) tibial components of an ankle joint coated by DLC [Hauert R., 2004].

The key issue in biocompatible coatings is their capability to prevent any rejection from the human body, i.e. avoid the formation of thrombus in blood due to an abnormal interaction and adsorption of proteins. DLC shows acceptable bio- and hemocompatibility, since the low platelet adhesion on coated implants points to a weak rejection. This led to commercial launch of heart valves.

Regarding joint coatings, the graphitic transfer layer is not built up on the soft counterpart from UHMWPE/DLC interface when operating in biological media. This lack of protection promotes wear on the organic surface. Further tests have confirmed that DLC/DLC systems in biological environments have a successful behaviour, and showed that the residual graphite from the transfer layer is tolerated by the body. However, in vitro experiments performed on joints show particularly contradicting results mainly due to the experimental setups of simulations (ball-on-disk, hip simulator). Their results are very sensitive to the used instruments and lubricants.

Due to the amorphous structure of DLC, other elements can be added to tailor its properties, as for instance the chemical response in front of certain environments. Si:O incorporation shows a reduction in inflammatory processes, and the behaviour of other DLC-alloys is currently investigated. Me-DLC nanocomposites consisting in DLC-Ag-Pt systems have been recently developed by PLD processes. Functionally gradient multilayers

of DLC and hydroxyapatite ($Ca_{10}(PO_4)_6(OH)_2$) constitute other examples of nanostructured DLC films investigated for medical applications [Narayan R.J., 2005].

In the context of medical applications, surgical instruments as needles and guidewires also take advantage of the special mechanical properties of DLC.

2.3.7. Sport equipment

As a tribological application in sports area, we find DLC coated golf club heads [Hauert R., 2004]. The expected effect is to minimise spin of the ball thanks to the absence of friction force when the club hits the ball.